the
abdus salam
international centre for theoretical physics

SMR: 1098/11

WORKSHOP ON THE STRUCTURE OF BIOLOGICAL MACROMOLECULES

(16 - 27 March 1998)

"DNA Bending"

presented by:

Sandor Pongor

International Centre for Genetic Engineering and Biotechnology (ICGEB)
Protein Structure and Function Group
Padriciano, 99
I-34012 Trieste
Italy

ROD MODELS OF DNA: SEQUENCE-DEPENDENT ANISOTROPIC ELASTIC MODELLING OF LOCAL PHENOMENA

Mircea Gh. Munteanu[1], Kristian Vlahovicek[1], Subbiah Parthasarathy[1], István Simon[2] and Sándor Pongor[1]

[1]International Centre for Genetic Engineering and Biotechnology
Padriciano 99, 34012 Trieste, Italy, pongor@icgeb.trieste.it

[2]Institute of Enzymology, BRC, Hungarian
Academy of Sciences, H-1518 Budapest P.O.Box 7, Hungary

Keywords:

DNA bending, DNA models, DNA curvature, Finite element method, Internet server

Corresponding author:

Sándor Pongor
International Center for Genetic Engineering and Biotechnology
Padriciano 99, 34012 Trieste, Italy
Tel: +39 40 3757300
FAX: +39 40 226 555
E-mail: pongor@icgeb.trieste.it

Abstract

Local DNA bending can be predicted by simple static geometry models as well as by elastic models that incorporate sequence dependent anisotropic bendability (SDAB). In addition, the SDAB model qualitatively explains phenomena including affinity of protein binding, kinking, and sequence-dependent vibrational properties of DNA. A www server is available at www.icgeb.trieste.it/net.

Introduction

The possibility that DNA may contain localized conformational signals, in addition to the information stored in the base sequence,has profoundly influenced the thinking of biologists in recent years. DNA is no longer considered a straight, featureless double helix but rather a series of individual domains differing in flexibility and curvature. This local structural polymorphism can extensively contribute to the specificity of such biological events as gene regulation, and packaging, for example, through regulating the affinity of protein binding[1]. In contrast to traditional structural polymorphism (e.g. B, A or Z structures), here we deal with a localized micropolymorphism in which the original B-DNA structure is only distorted but is not extensively modified. Broadly speaking, the DNA segments involved in protein-induced and inherent DNA-bending are 10-50 base pairs in length,[2] i.e. they are longer than what can be easily handled by atomic resolution molecular modelling or quantum mechanical approaches. Traditional elastic models of DNA, that represent DNA as an ideally elastic, homogeneous cylindrical rod, were used to model macroscopic behaviour of long DNA segments, such as supercoiling[3, 4]. However, local DNA conformations and recognition by DNA-binding proteins are clearly sequence-dependent, so conventional elastic rod models of DNA, which do not explicitly represent the dependence of the elasticity on the base sequence, cannot tell us much about them. Here we attempt to briefly review advantages and limitations of the rod-models of DNA with particular regard to elastic modelling of local bending phenomena.

Static geometry models

Rod models are the simplest form of DNA models that picture DNA as a cylindrical rod of constant diameter. The shape, in this case, is the path or trajectory of the longitudinal axis, which can be either straight or curved. (**Figure 1A**). The common philosophy of rod models is to divide the rod into short cylindrical segments (e.g. of the size of a base

pair) and then to compute some rod parameter based on the segment parameters that have to be known *a priori* . Dinucleotide models define the base pair-size unit as one between two adjacent base pairs, which results in 16 different base pairs, or 10, if we allow strand symmetry (i.e. AA=TT). Trinucleotide models define the unit around the base pair in the middle of a given trinucleotide. This amounts to 64 or 32 different units, again depending on strand symmetry.

Static models are rigid rod models that only consider the static geometry of a constituting segment. Curvature in B-DNA was originally believed to be an attribute of A_n (n=4-6) tracts repeated in phase with DNA's helical repeat. Two static models have been proposed initially to explain the phenomenon. In the nearest neighbour model, the axial deflections of successive AA/TT dinucleotides add up to produce a curve[5]. In the so-called junction model, curvature is produced as the modified B-DNA structure of A_n tracts joins with adjacent B-DNA[6]. More recently it became clear that in addition to the A_n tracts, DNA curvature involves additional sequence elements[7, 8], and more sophisticated models were proposed which included wedge angles for all 16 dinucleotides[9, 10].

Current static models consider dinucleotide geometries derived from direct measurements such as X-ray crystallography[11, 12] and NMR[13, 14], from statistics of nucleosome binding data[7, 15] or from gel electrophoretic analysis of concatenated synthetic oligonucleotide repeats [9, 10] . The parameters explicitly considered are Roll, Tilt and Twist angles, and all other parameters are considered equal to that of B-DNA (the diameter of the rod plays no role in this calculation). Given the geometry of the segments one can calculate the trajectory of DNA by adding the distortions of the successive segments. This exercise is only seemingly simple, because the addition of rotation operations like roll, tilt and twist are not commutative, so the results in principle depend on the serial order of the operations[16]. The resulting error is negligible for short DNA segments and for small angles (and generally speaking, roll and tilt angles are small). The calculation will however give large uncertainties for long segments or for large

distortions. There are a number of programs available that can calculate an approximate DNA trajectory starting from a DNA sequence [10, 12, 17-19]. The clue to most approximations is that if the angles are small, then they can be approximately added as vectors (**Figure 1B**). This approximation again, is valid only for short segments. Table 1 shows that the current dinucleotide models give good qualitative correlations with the known experimental values, i.e. curved and straight motifs can be distinguished even though all models mispredict some of the motifs. It has to be mentioned that the gel mobility anomaly of DNA that is used to validate the models is itself strongly dependent on environmental factors such as metal salts and temperature, so our knowledge on straight and curved motifs is qualitative rather than quantitative.

Simple elastic models

If a rod is ideally elastic one can compute the energy necessary for bending, stretching or torsional deformation[20]. For example, the energy required to bend the rod of length L to a given curvature can be calculated as

$$\Delta G = \frac{1}{2} EIL\alpha^2. \qquad [1]$$

Here α is the curvature as defined in **Figure 1A** and I is the moment of inertia that, for a cylindrical rod of r radius is given as $\pi r^4/4$. E is the stiffness parameter or Young's modulus. Based on a variety of physico-chemical measurements and direct molecular stretching studies, the stiffness (Young's modulus) of average DNA is about of 3.4 x 10^8 N/m^2, a value close to that of polypropylene or phenol resins.

By "simple elastic models" we mean those that consider DNA as an originally straight cylindrical rod with one *homogeneous isotropic elasticity* parameter (for extensive reviews see[2, 4, 21]). This means, on one hand, that the model is not sequence

dependent, i.e. all segments are equal, and, on the other, that the model is equally bendable (deformable) in all directions. The phenomena that can be described with such a simplified elastic model include the gross shape changes of DNA like supercoiling, response of plasmids to stress, etc. The nature of the answer is qualitative. For example one can state that the shape of a plasmid-like elastic ring model adopts, in response to torsional stress, shapes that are reminiscent of the shapes observed for supercoiled plasmids. This fact shows that some properties of DNA are in fact reminiscent of those of rubber strings, i.e. they depend mostly on properties that are common to simple mechanical systems. The underlying, quite complex mathematics can be avoided by *finite element analysis*, a technique routinely used for the analysis of deformations in engineering[22]. This technique has been applied with success for small DNA deformations[23, 24]. Even though simple elastic models do not contain local (i.e. sequence dependent) information, they allow, on the other hand, to demonstrate how local structures might act on the elastic behaviour of the entire molecule. For example, incorporating a fixed curve into a DNA model will influence the gross shape of plasmids[25] and will bring distant sites into each other's vicinity[26].

Anisotropic, sequence dependent elastic models

In order to model local phenomena starting from a base sequence, one has to incorporate sequence dependence into the elastic models. It is also known that bending is anisotropic[27, 28], i.e. DNA bends much more easily towards the major groove than in any other direction, moreover, bending in the tilt direction is not favourable in energetic terms (for a review see[2]). We have developed anisotropic bendability parameters using the enzyme DNAse I[29]. This enzyme bends DNA towards the major groove and binds virtually to all DNA sites without a pronounced sequence specificity. DNAse I cutting rates can thus be used as an estimate of DNA bendability which can in turn can be scaled to an approximate DNA rigidity scale[30]. The result is a simplified segmented rod model, shown in **Figure 1C**. In this *sequence dependent anisotropic bendability* (*SDAB*), each

disk corresponds to one base pair and the arrow indicates the direction of facilitated flexibility (i.e. that of the major groove). In principle, such an anisotropic bendability model can have different bending flexibility in all directions. As a simplification, we take bendability towards the major groove as the principal parameter, and consider that DNA is 10-times stiffer in all other directions. The model does not include static deflection components, i.e. similar to isotropic models, it considers DNA as an originally straight rod. Nor does the model incorporate torsional flexibility. In other terms it is a stripped down model that is designed to reflect one aspect: local bending phenomena. In contrast to the isotropic elastic models, the SDAB model is non-linear in terms of displacement response, but is still amenable to finite element analysis.

Modelling of minicircles of curved and straight DNA[31] A simple experiment shows the macroscopic anisotropy of the SDAB model (**Figure 3**). A rod model is circularized into a minicircle (a) which is then writhed around (b) and the energy of the model is determined by finite element methods as a function of the rotation angle (c). Sequences that are repeats of curved DNA motifs, in fact, will have a rotational preference, i.e. there will be one stable energy minimum (**Figure 3**). This means that such a rod-model has a preferred direction of bending, so as a result of thermal fluctuations it will preferentially bend into one direction. In other terms, the physically measurable average conformation of such a model will be curved. The straight motifs, on the other hand, have either no minima or have two minima in opposite angular directions.

Another consequence of the energy minimum found in the circles is that, in the minimum energy conformation of helically phased repeats, certain motifs will face inwards and others outwards. For example, in repeats of AAAAGGGCCC, the GGGCCC motif faces inwards and the AAAAA are on the outer side of the circle. The roll values at the central GC are the highest while there are slight negative rolls in the AAAAA tract. As the roll/twist profile of the lowest energy conformation illustrates, the shape of the circle is reminiscent of a polygon - in fact quite similar to those recently obtained for the same

molecule using AFM microscopy[32]. This means that the lowest energy conformation has slight kinks which is reminiscent of the minikink model postulated by Zhurkin and co-workers[28]. The high energy conformers, on the contrary, have smaller kinks (not shown).

Protein/DNA binding: DNA rigidity versus complex stability[33] Repressor proteins bind to short DNA motifs with high specificity and the DNA is often bent in the resulting protein/DNA complex since bending is induced by the binding of the protein. If this is the case, the rigidity of the operator DNA can be expected to play a role in the binding. By plotting the experimental free energy values against the rigidity of the oligonucleotides (**Figure 4**) we find that cognate (operator) and non-cognate (non-operator) DNA follow two adverse, quasi-linear relationships. In the operator sequences, ΔG is higher for stiffer molecules , i.e. the stiffer the molecule, the weaker the binding. This, in fact, can be expected since Cro has to curve the molecule, and the energy required is linearly proportional to the stiffness [eqn 1].

In non-operator sequences, on the other hand, ΔG is lower for stiffer sequences, i.e. the stiffer the sequence, the stronger the binding. For the explanation of this phenomenon we consider a simple model (**Figure 3**, inset) in which Cro first binds to the oligonucleotide in a non-specific manner and reduces the free movement (thermal fluctuations) of DNA, which results in an entropy loss. Since the elastic entropy can be calculated from the $\langle\theta\rangle^{1/2}$ root mean square fluctuations of the model, the entropy change can be calculated as

$$\Delta S = nR\ln\left[\frac{\langle\theta^2_{bound}\rangle^{1/2}}{\langle\theta^2_{free}\rangle^{1/2}}\right] = nR\ln\left[\frac{E_{free}}{E_{bound}}\right], \qquad [2]$$

where E_{free} is the average Young's modulus of the segment, n is the number of degrees of freedom and E_{bound} is the Young's modulus of the bound (quasi immobilized) DNA. Since E_{free} is smaller than E_{bound}, this equation shows an adverse relationship, similar to

that shown in **Figure 3** (red line), which is in fact very near to linear in the range of the experimental data. In other terms, the relationship shown in **Figure 3** is qualitatively explained by the entropy loss, in accordance with the intuitive expectation that the "immobilization" of a stiff DNA cognate will take less energy on binding. The free energy change of the second step will have two components: that of the specific interaction (energy gain) and that of bending. Bending energy can be calculated according to equation [1] and it is directly proportional to the rigidity of DNA. **Figure 3** in fact shows that the complexes of more rigid DNA molecules are less stable. The slope of the curve corresponds to a curvature actually found in the crystal structure[33].

Prediction of bendable and curved segments Given the fact that the bendability of the SDAB model is asymmetrically facilitated towards the major groove, thermal fluctuations will result in bending the model. Bendability values in **Table 1** can be considered proportional to (but not identical with) static trinucleotide roll values, i.e. the bendability parameters can be considered analogous to a static geometry model based on trinucleotides. This fact is best illustrated by helical circle diagrams (**Figure 4A**) - a technique originally developed for amphipathic α-helices in proteins. In these diagrams, the bendability values are plotted on a plain as vectors pointing towards the major groove of each base pair. In randomly chosen DNA segments these plots are close to symmetrical with a vector sum close to zero. In curved DNA, the plots are asymmetrical and there is a substantial resulting vector. Based on this observation, the length H of this vector can be regarded as a measure of *curvature propensity*:

$$H = \frac{1}{n}\left[\left(\sum_{i=1}^{n} f_i \cos(i\omega)\right)^2 + \left(\sum_{i=1}^{n} f_i \sin(i\omega)\right)^2\right]^{1/2} \qquad [3]$$

where f_i is the bendability parameter for position i, ω is the twist angle (36° for ideal B-DNA) and n is the number of vectors in the segment (usually a segment length of 32 residues, i.e. approximately 3 helical turns are used for the calculation). It is interesting to

note that equation 3 is analogous to the hydrophobic moment of Eisenberg[34]. The SDAB model gives comparable predictions to the static geometry models (**Table 1**). Originally, equation [3] was used with the DNAse I-derived bendability data. **Table 1** also includes figures calculated with the so-called consensus bendability scale[14] which was developed in order to increase the sensitivity of the prediction towards GC-based curved motifs - these are often mispredicted with the static dinucleotide models[15].

Since the *SDAB* model includes the prediction of bendability parallel to curvature, it allows one to distinguish rigid, flexible and curved segments of a molecule using one and two-dimensional plots (**Figure 4B,C,D**). The latter can be especially useful in evaluating longer sequences, such as genomes (**Figure 5**).

Conclusions and future directions

We can conclude that static and dynamic rod models describe different aspects of the DNA molecule with as few parameters as possible. If they succeed - and they do, quite surprisingly - it means, that the parameters used by the model sufficiently explain a given aspect of the molecule's behaviour. Both type of models can predict curvature in short DNA segments - in this respect they can be considered equivalent.[35] The differences in predictive accuracy may be due to the parametrisation (e.g. trinucleotide vs. dinucleotide representation, electrophoresis vs. nucleosome data, etc.) and not to the models themselves. Considering the significance of these structural features, it is worth mentioning that bendability/curvature characteristics are conserved in evolutionarily[31, 36] and functionally related sequences[37], and they correlate well with regulatory sites known from experiment[38]. The *SDAB* model also makes it possible to study the sequence-dependent vibrational characteristics of DNA (**Figure 6**). This is primarily important since sequence dependent vibrational differences may be responsible in promoting or blocking energy flow along the DNA molecule.

Refinements of the rod models, especially the incorporation of tetranucleotide-based description will probably increase the predictive accuracy and increase the scope of applications. Future models may combine both static and dynamic features with particular reference to the principles of non-linear DNA dynamics[39] . At the same time molecular mechanic models are also expected to expand to a wider range of local phenomena as illustrated recently by Lavery and associates[40]. In the foreseeable future however, the simple rod models will continue to play a key role in the large scale analysis of genomic data.

Acknowledgements Thanks are due to Dr. J. Langowski and A. Bolshoy for advice. M.M.G. acknowledges the support of the Universitatea Transilvania, Brasov, Romania.

Table 1 Analysis of curved and straight sequence motifs with various methods[31]

No.	Sequence motif	Static geometry model				Sequence dependent anisotropic bendability (SDAB) model			
		Curvature [degree/helical turn]				Bendability [a.u.]		Curvature propensity [degree/helical turn]	
		Bolshoy et al, elfo [9]	Olson et al, X-rays[41]	Ulyanov & James NMR [13]	Nucleo-some 7, 15	DNAseI 29	Consensus [14]	DNAseI 29	Consensus [14]
	Curved DNA								
1	$(aaaattttgc)_n$	26.2	6.9	18.3	13.7	2.8	2.4	21.1	17.4
2	$(aaaattttcg)_n$	21.0	3.8	3.8	17.7	2.2	2.3	16.6	17.2
3	$(tctcaaaaaacgcgaaaaaaccggaaaaaagc)_n$	27.1	8.2	16.7	17.1	3.2	3.2	15.4	15.9
4	$(ccgaaaaagg)_n$	14.7	6.8	13.1	23.3	3.9	4.3	17.1	20.2
5	$(tctctaaaaaatatataaaaa)_n$	27.8	3.0	7.5	10.9	4.5	3.2	27.6	18.5
6	$(ggcaaaaaac)_n$	26.8	12.0	20.1	20.4	3.2	3.3	19.2	19.5
7	ccaaaaatgtcaaaaaataggcaaaaaatgcc - *L.tarentolae* kinetoplast	26.0	6.4	15.7	19.6	3.9	3.5	21.8	20.5
8	aaaaactctctaaaaactctccctagaggggccctagagggc	19.4	7.8	10.6	13.3	5.2	4.6	13.6	12.8
9	aaaaactctctaaaaactctctagaggggccctagagggccc	17.5	7.2	13.1	16.4	5.1	4.6	13.3	13.2
10	agaattgggacaaaaattggaaatttttaaggg - *C.risortia* bent satellite DNA	18.5	8.9	8.7	12.4	3.3	3.0	13.5	12.6
11	$(aaaaactctctaaaaactctcgaggggccctagagggccta)_n$	21.6	5.2	10.1	14.5	5.0	4.7	13.8	10.8
	Straight DNA								
12	$(atctaatctaacacaacaca)_n$	0.8	0.5	2.7	1.2	5.1	4.4	0.8	0.8
13	actacgttaaatctatcaccgcaagggataaa - OR3 operator region	10.4	5.5	4.9	5.9	5.0	4.4	10.4	7.8
14	actacgttaaatctatcaccgcaagggataaa - OR3 region, mutated	11.0	5.5	3.4	6.2	4.9	4.4	10.6	8.1
15	$(a)_n$ - poly-A [2]	0.008	0.000	0.008	0.000	0.100	0.063	0.002	0.002
16	$(ttttaaaacg)_n$	1.5	7.1	14.5	10.7	2.8	2.5	2.3	4.2
17	$(ttttaaaagc)_n$	1.7	0.8	16.0	16.3	3.6	3.3	3.0	9.6
18	$(aaaaactctctaaaaactctcgggccctagaggggccctaga)_n$	27.1	3.1	5.9	7.5	4.9	4.6	12.8	8.3

[1]The angular deflection [degree per helical turn of 10.5bp] was calculated by the www-server (www.icgeb.trieste.it/net). (The curvature units of Trifonov et al. corresponst to 4.5 °/bp or 47.25 °/10.5 bphelical turn).

References

1 Travers, A. A. and Klug, A. (1990) in *DNA topology and its biological effects* (Cozzarelli, N. R. a. W., J.C., ed.), pp. 57-106, Cold Spring Harbor laboratory

2 Olson, W. K. and Zhurkin, V. B. (1996) in *Biological Structure and Dynamics (Vol. 2)* (Sarma, R. H. and Sarma, M. H., eds.), pp. 341-370, Adenine Press

3 Olson, W. K. (1996) *Curr Opin Struct Biol* 6, 242-56

4 Langowski, J. *et al.* (1996) *Trends Biochem Sci* 21, 50

5 Trifonov, E. N. and Sussman, J. L. (1980) *Proc Natl Acad Sci U S A* 77, 3816-20

6 Wu, H. M. and Crothers, D. M. (1984) *Nature* 308, 509-13

7 Satchwell, S. C., Drew, H. R. and Travers, A. A. (1986) *J Mol Biol* 191, 659-75

8 Brukner, I. *et al.* (1993) *Nucleic Acids Res* 21, 1025-9

9 Bolshoy, A., McNamara, P., Harrington, R. E. and Trifonov, E. N. (1991) *Proc Natl Acad Sci U S A* 88, 2312-6

10 De Santis, P., Palleschi, A., Savino, M. and Scipioni, A. (1990) *Biochemistry* 29, 9269-73

11 Olson, W. K. *et al.* (1995) *Biophys Chem* 55, 7-29

12 Bansal, M., Bhattacharyya, D. and Ravi, B. (1995) *Comput Appl Biosci* 11, 281-7

13 Ulyanov, N. B. and James, T. L. (1995) *Methods Enzymol* 261, 90-120

14 Gabrielian, A. and Pongor, S. (1996) *Febs Lett* 393, 65-8

15 Goodsell, D. S. and Dickerson, R. E. (1994) *Nucleic Acids Res* 22, 5497-503

16 el Hassan, M. A. and Calladine, C. R. (1995) *J Mol Biol* 251, 648-64

17 Wheeler, D. (1993) *Biochem Biophys Res Commun* 193, 413-9

18 Shpigelman, E. S., Trifonov, E. N. and Bolshoy, A. (1993) *Comput Appl Biosci* 9, 435-40

19 Dlakic, M. (1998) *Bioinformatics* , in press

20 Barkley, M. and Zimm, B. (1979) *J. Chem. Phys* 70, 2991-2997

21 Vologodskii, A. V. and Frank-Kamenetskii, M. D. (1992) *Methods Enzymol* 211, 467-80

22 Zienkiewicz, O. C. and Taylor, R. L. (1991) *The finite element methods*, McGraw-Hill

23 Bauer, W. R., Lund, R. A. and White, J. H. (1993) *Proc Natl Acad Sci U S A* 90, 833-7

24 Yang, Y., Tobias, I. and Olson, W.K. (1993) *J. Chem. Phys.* 98, 1673-1686

25 Zhang, P., Tobias, I. and Olson, W. K. (1994) *J Mol Biol* 242, 271-90

26 Rippe, K., von Hippel, P. and Langowski, J. (1995) *Trends Biochem Sci* 20, 500-6

27 Schellman, J. A. (1974) *Biopolymers* 13, 217-26

28 Zhurkin, V. B., Lysov, Y. P. and Ivanov, V. I. (1979) *Nucleic Acids Res* 6, 1081-96

29 Brukner, I., Sanchez, R., Suck, D. and Pongor, S. (1995) *Embo J* 14, 1812-8

30 Gromiha, M. M., Munteanu, M. G., Gabrielian, A. and Pongor, S. (1996) *J. Biol. Phys.* 22, 227-243

31 Gabrielian, A. *et al.* (1997) in *Biomolecular Structure and Dynamics* (Sarma, R. H. and Sarma, M. H., eds.), Adenine Press, Inc.

32 Han, W., Lindsay, S. M., Dlakic, M. and Harrington, R. E. (1997) *Nature* 386, 563

33 Gromiha, M. M., Munteanu, M. G., Simon, I. and Pongor, S. (1997) *Biophysical Chemistry* 69, 153-160

34 Eisenberg, D., Schwarz, E., Komaromy, M. and Wall, R. (1984) *J Mol Biol* 179, 125-42

35 Calladine, C. R. and Drew, H. R. (1996) *J Mol Biol* 257, 479-85

36 Gabrielian, A., Simoncsits, A. and Pongor, S. (1996) *Febs Lett* 393, 124-30

37 Schatz, T. and Langowski, J. (1997) *Journal of Biomolecular Structure and Dynamics* 15, 265-275

38 Langst, G., Schatz, T., Langowski, J. and Grummt, I. (1997) *Nucleic Acids Res* 25, 511-7

39 Yakushevich, L. V. (1994) *Physica D* 79, 77-86

40 Sanghani, S. R., Zakrzewska, K., Harvey, S. C. and Lavery, R. (1996) *Nucleic Acids Res* 24, 1632-7

41 Gorin, A. A., Zhurkin, V. B. and Olson, W. K. (1995) *J Mol Biol* 247, 34-48

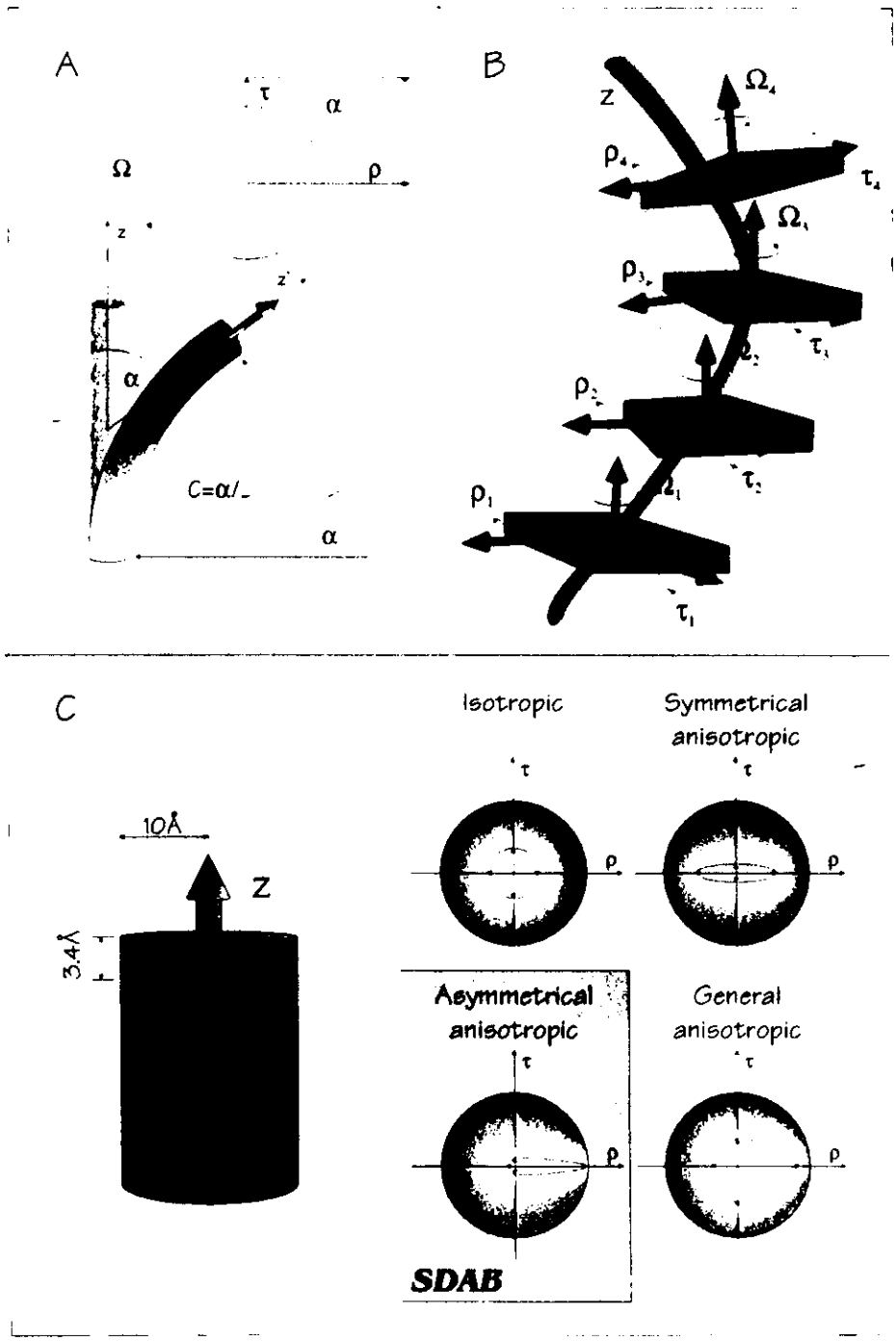

Figure 1 A Curvature of a rod and relationship with DNA geometry parameters. **B** Schematic calculation of trajectory using a static geometry model. The deflection is approximately the vector sum of the dinucleotide geometries (r_ρ, τ, Ω vectors), as shown in **A**. **C** Sequence-dependent anisotropic bendability models of DNA. Each element corresponds to one basepair. The arrow in each basepair schematically indicates the direction pointing towards the major groove. The arrows are proportional to the flexibility in a given direction (+x, -x, +y, -y). In the SDAB model, one direction (that of the major groove) is more flexible, the other three are more rigid[30].

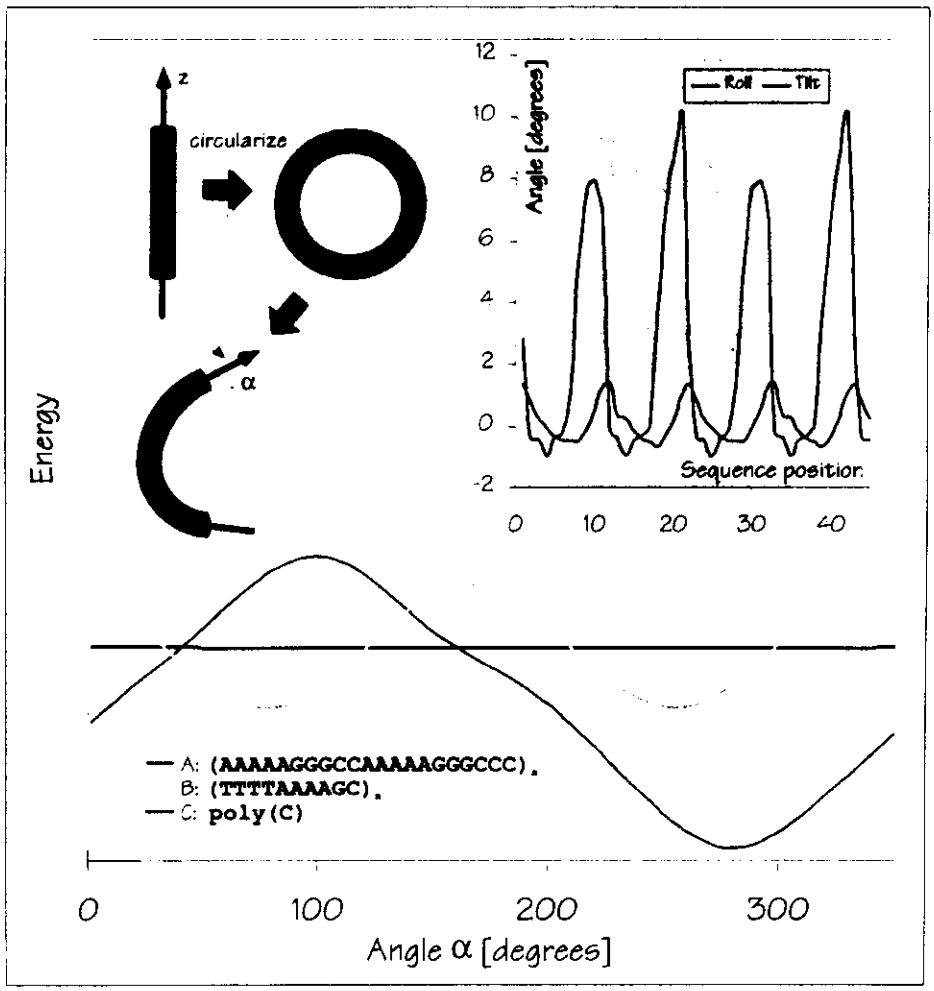

Figure 2 Testing bending anisotropy in DNA by finite element methods. A DNA model was built (as outlined in **Figure 2**) from the repeat motifs shown as inset . The models were bent into a circle and the circle was twisted around the now circular z-axis, as shown (inset). The energy of the model was calculated by finite element methods and plotted as a function of the angle of twisting. Curved motifs (e.g. A^{32}) exhibit a single energy minimum, i.e. clear bending preferences in one direction. Straight motifs have either no minimum or minima in two opposite directions (B,C)[31].

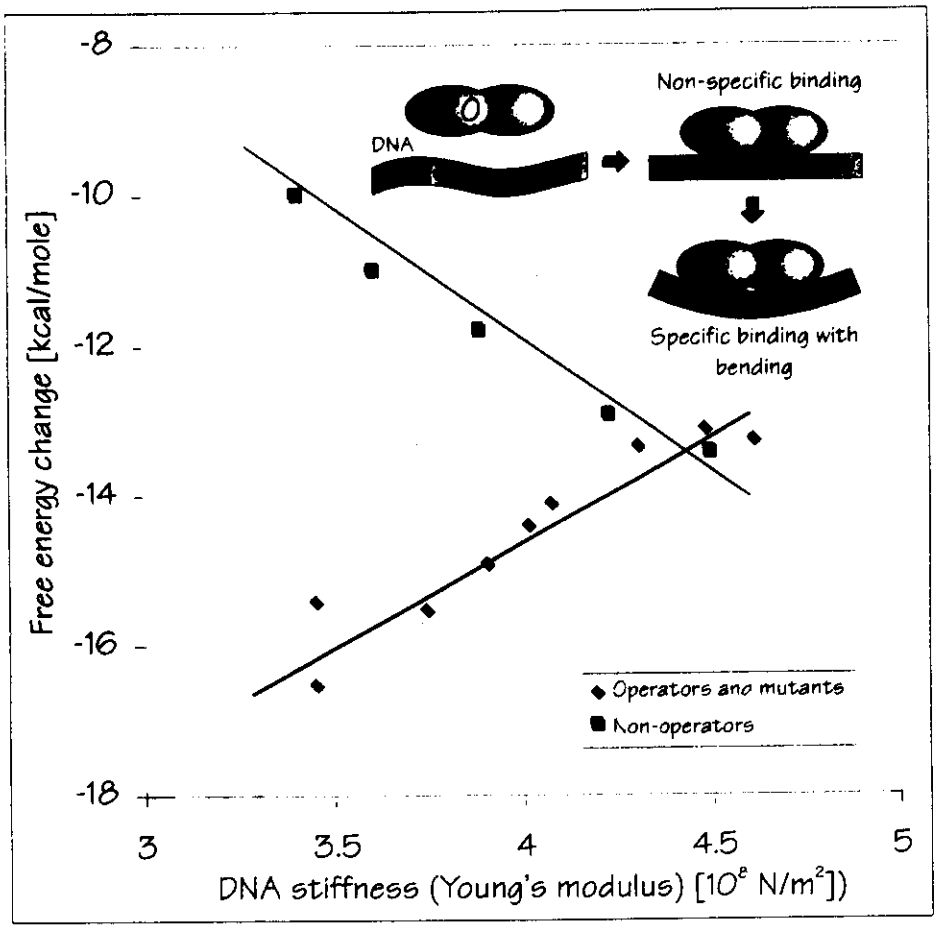

Figure 3 Binding of Cro operator to oligonucleotides of different stiffness. Relationship between the average stiffness (Young's modulus) of DNA and the free energy change (ΔG) of operator (blue) and non-operator (red) DNA sequences.[33].

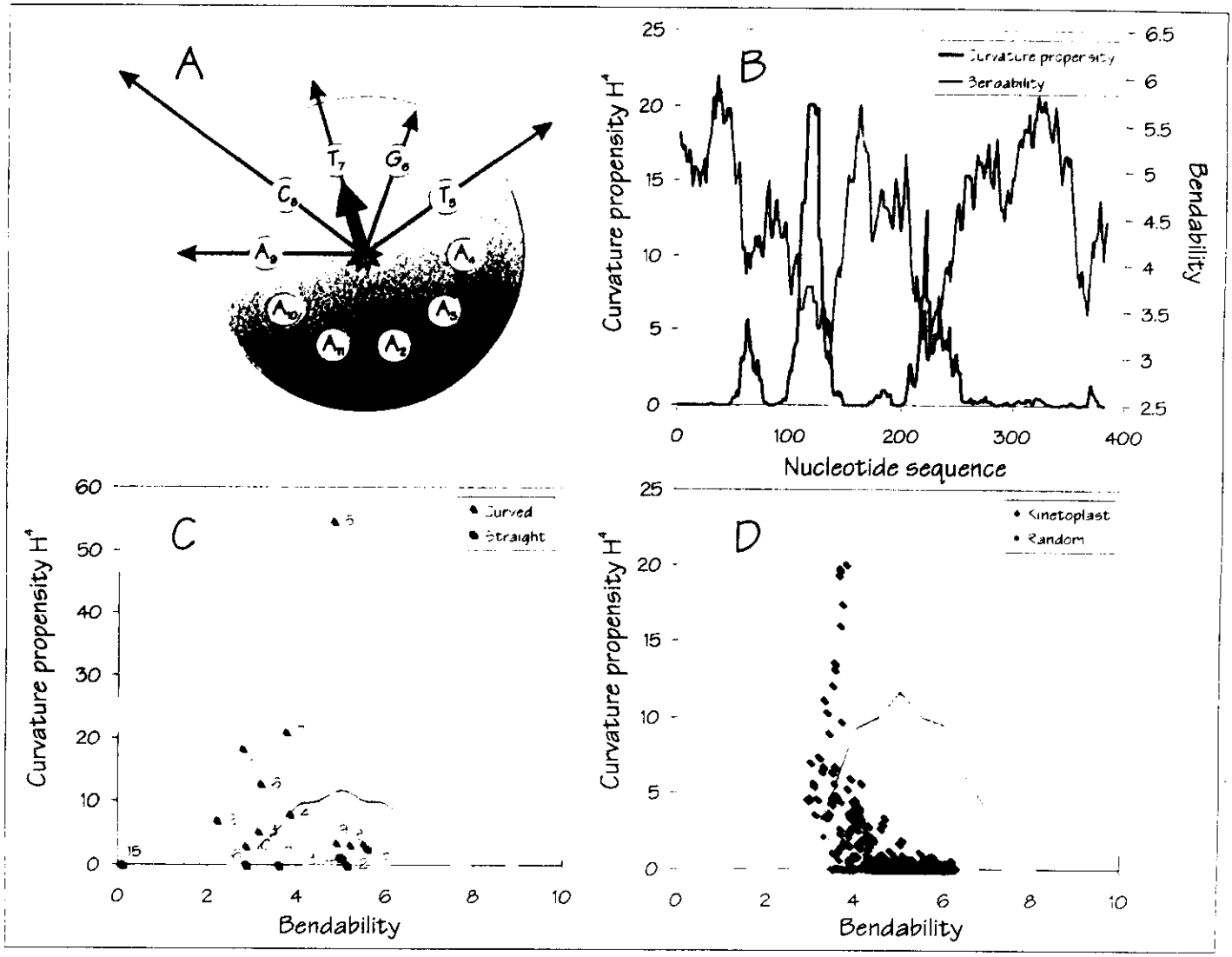

Figure 4 **A** Vectorial representation of bendability (helical circle diagram) in a curved sequence motif (A)AAATGTCAAA(A) from a *Leishmania tarentolae* class II minicircle. The length of black arrows is proportional with that of the bendability parameter at the given sequence position. The red arrow is the vectorial average of the bendability vectors (given in equation [3]. **B**: Curvature propensity (Helical asymmetry) (red, equation [3]) and bendability (blue) versus sequence plot (Sequence: Genbank LEIKPMNC2). The blue dotted line indicates the average bendability value of DNA. **C**: Curvature vs. bendability plots. of Curved (red) and straight (blue) sequences from Table 1. The red and green dashes indicate the border of random sequences obtained by random-shuffling of the sequences of *H. influenzae* genome and yeast chromosome III., respectively. **D**:*Leishmania tarentolae* class II minicircle The values are calculated for 30 bp sequence segments.[36]

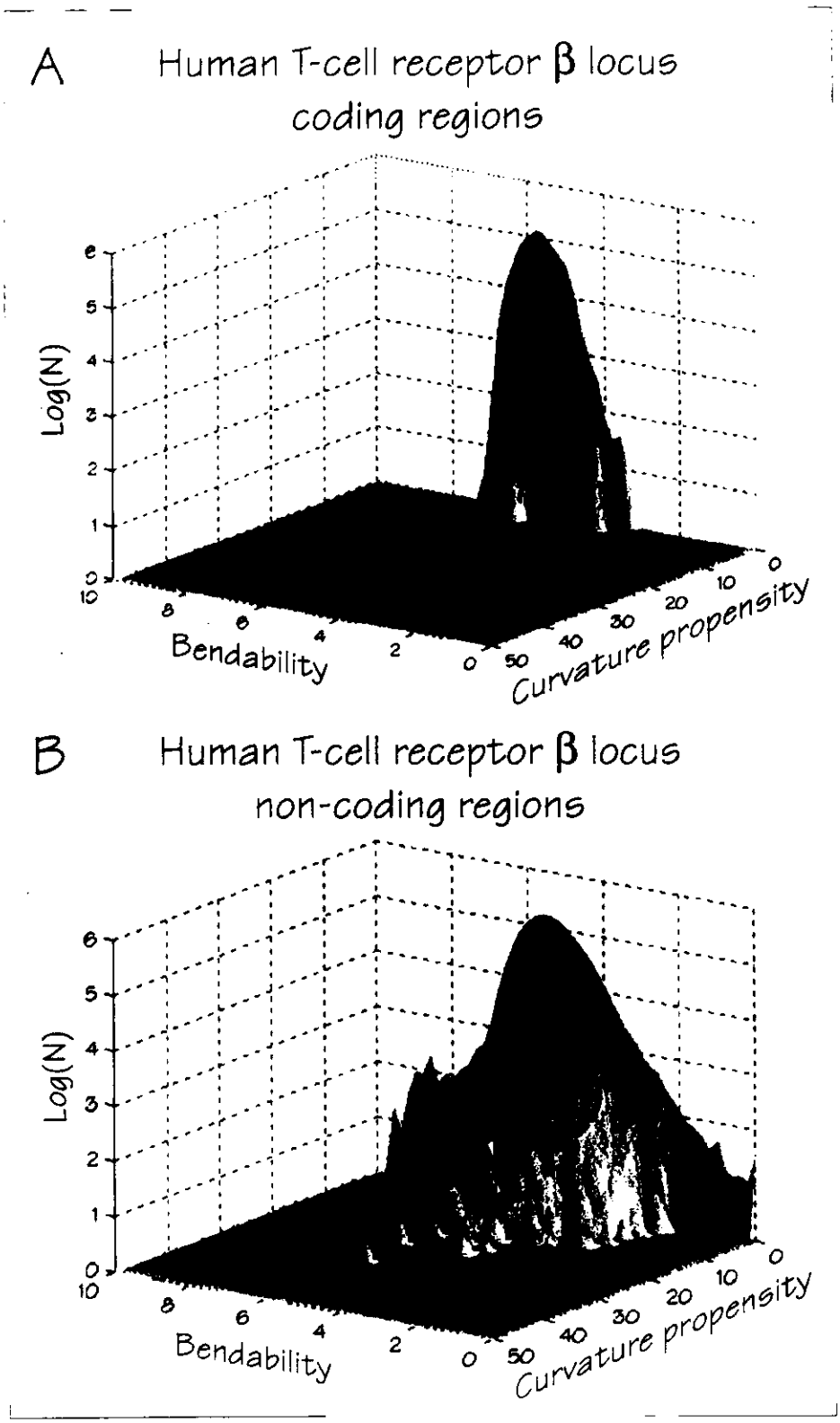

Figure 5 3D Curvature propensity (equation [3]) vs. bendability histogram of the Human T-cell receptor locus (Genbank: humtcrb). The protein coding regions (a) have a tight distribution around average bendability and low curvature. The non-protein-coding regions (b) have a higher number of stiff (low bendability), flexible and curved segments[31].

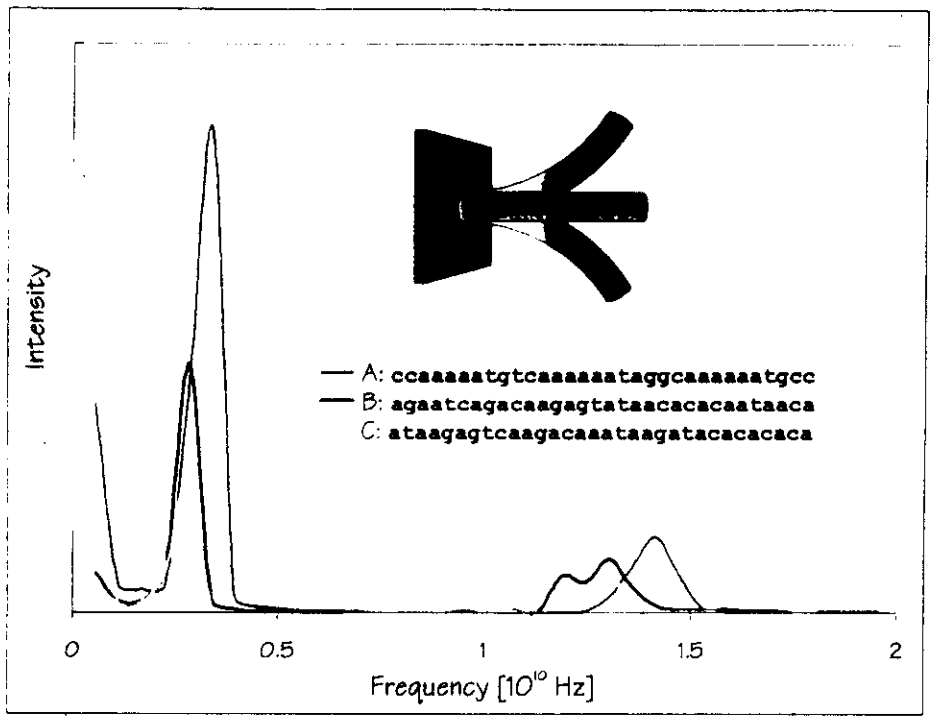

Figure 6 Sequence-dependent vibrations of DNA-models. A is an inherently curved sequence from *Leishmania tarantolae*, B and C are random shuffled variants of the same sequence, with no predicted curvature. A model of 32 residues was fixed on one end as shown in the inset and the free end was deflected to a moderate curvature of 7 degrees per helical turn and then left to vibrate. The movement of the free end was analyzed by Fourier analysis to give the frequency spectrum shown here.

Modeling superhelical DNA: recent analytical and dynamic approaches

Tamar Schlick

New York University and The Howard Hughes Medical Institute, New York, USA

During the past year, a variety of diverse and complementary approaches have been presented for modeling superhelical DNA, offering new physical and biological insights into fundamental functional processes of DNA. Analytical approaches have probed deeper into the effects of entropy and thermal fluctuations on DNA structure and on various topological constraints induced by DNA-binding proteins. In tandem, new kinetic approaches — by molecular, Langevin and Brownian dynamics, as well as extensions of elastic-rod theory — have begun to offer dynamic information associated with supercoiling. Such dynamic approaches, along with other equilibrium studies, are refining the basic elastic-rod and polymer framework and incorporating more realistic treatments of salt and sequence-specific features. These collective advances in modeling large DNA molecules, in concert with technological innovations, are pointing to an exciting interplay between theory and experiment on the horizon.

Current Opinion in Structural Biology 1995, 5:245–262

Introduction

The past decade has been an exciting time for nucleic acid enthusiasts. A surge of advances in both experimental and theoretical techniques has brought to light many intriguing structural properties of DNA — from the base pair (bp) level to higher organizational forms (supercoils, knots, catenanes, and protein–DNA complexes) — leaving behind the old-fashioned notion of a boring, ordered molecule. Progress in understanding these higher-order forms, in particular, leads to insights into fundemental functional processes of DNA that involve strand unwinding (replication, transcription) and passage (knotting and catenation), looping and slithering. A glimpse into the studies described in the proceedings of the Eighth Conversation in Biomolecular Stereodynamics, for example, indicates the diverse and growing body of work on nucleic acid structure [1••].

This article reviews recent analytical and numerical (simulation) work related to DNA supercoiling. The formation of supercoiled DNA involves twisting and bending of the DNA (Fig. 1) about its double-helical axis. When this wrapping process involves self interaction, like a braid, a plectoneme (interwound configuration) results (Fig. 1); if instead, the winding occurs around the imaginary axis of a torus, a toroidal superhelix is formed. Both modes of interwound supercoiling and the mode of DNA bound (and topologically constrained) to a protein matrix have profound biological significance. The linear sequence of the DNA carries the genetic information; the compact supercoiled state — which readily stores energy for essential biological processes — is an important functional state as well as a facilitator of regulation and of packaging with proteins; the yet more highly organized form in nucleoprotein complexes is an important storage form of the DNA (Fig. 1). Thus, progress in understanding DNA supercoiling, in particular, is important for a greater understanding of many fundamental biological processes, such as replication, recombination, and transcription. These reactions often require, or are facilitated by, a supercoiled DNA substrate.

The study of the many different levels of configuration of DNA is particularly challenging to modelers. The large size of DNA molecules (thousands of base pairs) and the large spatial scales and time ranges associated with their folding make for a formidable computational challenge. Indeed, supercoiling can condense the DNA by several orders of magnitude, and a wide range of characteristic timescales is associated with configurational rearrangements and hydrodynamic properties of supercoiled DNA. Thus, high-speed computers are natural vehicles to tackle this modeling challenge. Furthermore, experimental information on structure is coarse on the level of plasmids, in contrast to the atomic description on the oligonucleotide level available for a steadily increasing set of crystallographically determined structures [2]. The coarseness of structural data on the scale of whole molecules makes verification of models for DNA supercoiling difficult.

bp—base pair; MD—molecular dynamics.

 ISSN 0959-440X

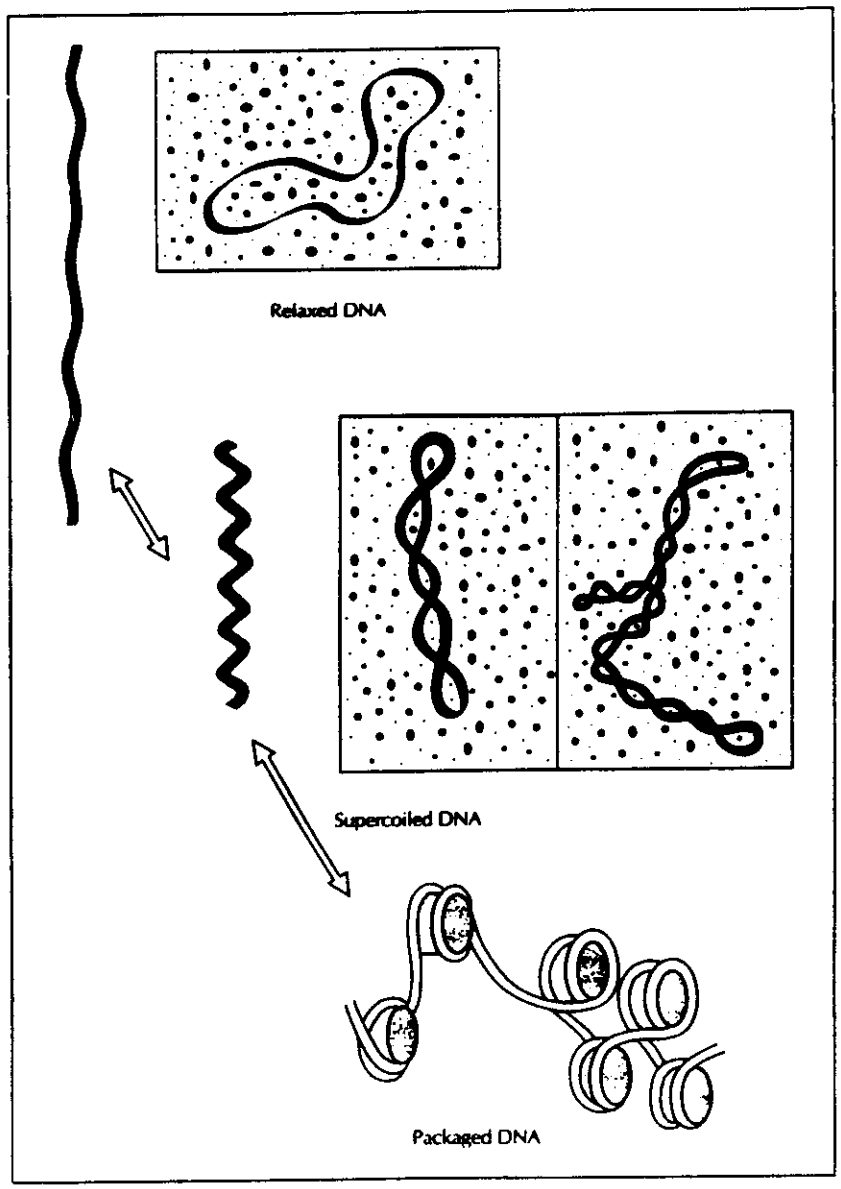

Fig. 1. A subjective view of the structural hierarchy of DNA. Linear or relaxed circular DNA can become supercoiled upon the action of the enzymes known as topoisomerases. Supercoiled DNA is an important functional state active in the processes of replication, transcription, and recombination. (The images in boxes are cartoons of electron micrographs.) Higher organizational forms of the DNA, such as the protein–DNA complexes in the chromatin of higher organisms, are formed through interactions with special proteins and are an important storage state of the hereditary material.

Nonetheless, a variety of analytical and numerical approaches have been developed in recent years at various levels of detail, reflecting a broad range of interest in many aspects of DNA structure from the biological to the physical sciences. The richness of models and methods stems from the multidisciplinary nature of the subject. The study of DNA structure (encompassing its geometry and topology) and the relation of structure to function spans biology, mathematics, chemistry, and physics. The participationn of yet another discipline, computer science, has enabled the introduction of large-scale computer models, and adds another exciting dimension to these studies. These models have provided, and will undoubtedly continue to provide, valuable insights into the properties of supercoiled DNA, insights that cannot easily occur through work in the laboratory. Ultimately, perhaps, these theoretical efforts will culminate in an integration of macroscopic with microscopic descriptions of DNA. Atomic-level molecular mechanics and molecular dynamics (MD) simulations are now providing detailed descriptions of the microscopic behavior of DNA ([3•]; see also Brooks, this issue, pp 211–215). It is also likely that predictions of DNA structure and behavior from these new models will stimulate innovations in experimental techniques (e.g. new techniques in scanning force microscopy [4•]) that will permit a finer examination of the architecture of supercoiled DNA.

There are several excellent recent reviews on modeling nucleic acids. Malhotra *et al.* [5•] review unconventional (i.e. macroscopic) techniques for large nucleic acids, both DNA and RNA. Beveridge and Ravishanker [3•] review

all-atom MD simulations of DNA in the past decade. Vologodskii and Cozzarelli [6] summarize work focusing on large-scale structural properties of DNA, such as supercoiling, knotting, and looping, and separately review progress in theoretical and experimental studies of DNA supercoiling [7•]. Similarly, Levene [8] describes experimental and theoretical approaches for studying the conformations and energetics of supercoiled DNA and includes synopses of energy-minimization calculations, Monte Carlo methods, and MD simulations. This review focuses on selected aspects of analytical and simulation approaches applied to DNA supercoiling in the past year: analytical frameworks that incorporate entropic effects, analytical frameworks that have time-dependent extensions, and simulation approaches that focus on DNA kinetics. Thus, energy minimization studies, including finite-element analyses (equilibrium forms at a temperature of absolute zero), as well as (static) equilibrium-distribution approaches and experimental studies, will not be detailed here (see Table 1 for a list of current approaches). Background information on DNA supercoiling can be found in several textbooks and monographs [9–11,12••]; a lively, less technical introduction can be enjoyed in [13••].

The elastic rod model

The elastic energy approximation has proven valuable for studying global (i.e. collective motions that are long range and occur over relatively long time scales) features of superhelical DNA. Indeed, much theoretical progress has been made since the pioneering applications of Fuller [14,15]. In this model, the DNA polymer is idealized as a long, thin and naturally straight (i.e. no intrinsic curvature) elastic isotropic rod with a circular cross section (Fig. 2). Homogeneous bending (i.e. equal flexibility in all directions) is often assumed as a first approximation. Although preferential directions of bending into the major and minor grooves are certainly recognized for nucleic acids [16,17,18••,19•], the uniform elastic chain view is a reasonable first-order approximation for naturally occurring DNA of mixed sequences that are not intrinsically bent. The elastic deformation energy can then be written as a sum of bending and twisting potentials (E_B and E_T), with bending and torsional-rigidity constants (A and C, respectively) deduced from experimental measurements of DNA bending and twisting [20]. For example, A can be linearly related to the (bending) persistence length of the DNA, p_b, by: $A = k_B T p_b$ (k_B is Boltzmann's constant and T is the temperature) and to the root mean square (rms) bending angle $\langle \theta_b^2 \rangle^{1/2}$ of a semiflexible chain with a preferred axis of bending (perpendicular to the helix axis), for which the angular fluctuations are independent from one another, through the expression

$$A = \frac{2k_B T d}{\langle \theta_b^2 \rangle}, \qquad (1a)$$

where d is the distance between base pairs (around 0.34 nm) [20,21].

The choice of elastic parameters is important for several reasons. First, analytical results depend sensitively on the ratio $\rho = A/C$, which is related to both Poisson's ratio (σ_e) — a characteristic of a homogeneous isotropic material — and the geometry of the rod-cross section. Specifically, for a homogeneous elastic rod of circular cross-section, $\rho = 1 + \sigma_e$. Second, equilibrium structures

Table 1. Approaches for studying DNA supercoiling.

Approach	Techniques	References
Experiment	Gel electrophoresis, electron microscopy	[45••,49•]
	dynamic light scattering,	[46,56]
	scanning force microscopy, etc.	[4•,27]
Analytical	Mechanical elastic-rod equilibria:	[31••,33–35,43]
	Euler-angle, curvature-torsion representations	[37•,38•,39••,40•,47•]
Numerical energy minimization	Simulated annealing, finite elements,	[18••,23,36•,48•,57]
	deterministic minimization	[24,25•,41•,44]
Equilibrium distributions	Metropolis/Monte Carlo	[6,7•,8,50,51]
Dynamic	Molecular dynamics	[5•,52] (a,b)
	Langevin and Brownian dynamics	[24,25•,41•,54•,58•]
	dynamic elastic-rod simulations	[59•] (c)

The techniques listed in the second column are illustrative rather than exhaustive. The reference list only includes works cited in this review. (a) D Sprous, RK-Z Tan, SC Harvey, personal communication. (b) RK-Z Tan, D Sprous, SC Harvey, personal communication. (c) I Klapper, M Tabor, personal communication.

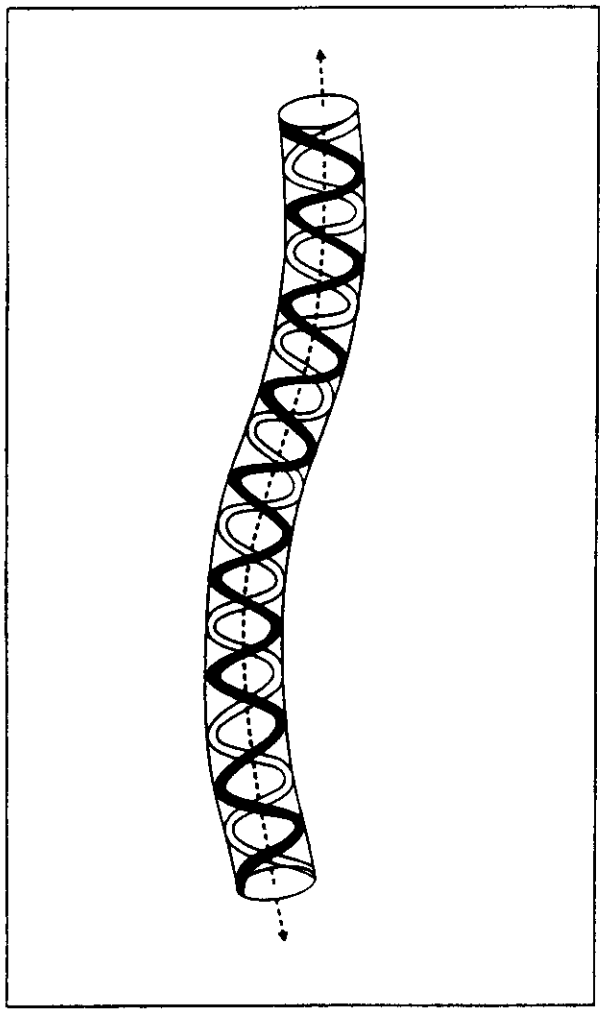

Fig. 2. An idealized representation of double-helical DNA as a long and thin elastic rod of circular cross-section. The rod is shown bent to illustrate a typical fluctuation from the straight resting state, as commonly found in interwound supercoiled DNA.

and profiles (collective descriptions) are considerably affected by the numerical values of A and C, which are linearly related to Young's modulus (E_c) of an elastic material [22]. Indeed, the configurational and energetic properties vary as A and C are altered (see [23,24], for example). Third, and perhaps most important, an adjustment of the standard elastic parameters is necessary when electrostatic interactions are modeled explicitly (e.g. using a Debye–Hückel term). This adjustment involves a bending constant A corresponding to the bending persistence length limit at high salt concentrations (see Table 2), in combination with a twisting coefficient that yields experimentally observed ranges of individual base pair twist fluctuations [25•].

In most DNA studies, the persistence length for bending is taken to be around 50 nm [20]. This corresponds to $A \approx 2.0 \times 10^{-19}$ erg cm and to $\langle \theta_b^2 \rangle^{1/2} = 6.7°$, at room T, in the context of isotropic bending. To relate the stiffness to measured standard deviations of DNA bending angles,

Table 2. DNA parameters•.

c_s(Na⁺)	p (nm)	A ($\times 10^{-19}$ erg cm)	$\langle \theta_b^2 \rangle^{1/2}$	d (nm)
1.0	31.7	1.28	8.4°	3.0
0.5	38.3	1.54	7.6°	3.4
0.2	46.9	1.89	6.9°	4.4
0.15	49.7	2.00	6.7°	4.9
0.1	53.5	2.15	6.5°	5.6
0.07	56.9	2.29	6.3°	6.8

•The persistence length p is estimated as a function of the molar sodium-salt concentration, c_s, according to the formula $p = 31.7 - 2.18 \log (c_s)$ [26]. The elastic bending constant $A = p(k_BT)$ ($k_BT = 0.04024$ to give the resulting units of A at 300 K). The root mean square bending angle is obtained from the relation $\langle \theta_b^2 \rangle^{1/2} = \sqrt{2(k_BT)d/A}$, where the effective DNA diameter $d = 0.34$ nm (yielding a value in radians with the constants above). The values of d as a function of c_s reported in the last column are obtained from Stigter [60]. The values of d at $c_s = 0.15$ and at 0.07 M are estimated from a curve based on Stigter's tabular values (see [25•] for details).

the two components of bending, namely roll (θ_{b1}) and tilt (θ_{b2}), each with associated stiffness constants A_1 and A_2 [18••], can be related to A through

$$A = \frac{2k_BTd}{\langle \theta_{b1}^2 \rangle + \langle \theta_{b2}^2 \rangle}. \qquad (1b)$$

Thus, the bending persistence length of 50 nm corresponds not only to an isotropic model where $\langle \theta_b^2 \rangle^{1/2} = 6.7°$, but also to an anisotropic bending model where $\langle \theta_{b1}^2 \rangle^{1/2} = 5.7°$ and $\langle \theta_{b2}^2 \rangle^{1/2} = 3.6°$; the last two measured values are obtained from static variational analysis of B-form DNA crystal structures [19•]. (Note that for sufficiently small angular deflections, $\langle \theta_b^2 \rangle = \langle \theta_{b1}^2 \rangle + \langle \theta_{b2}^2 \rangle = [k_BTd(A_1 + A_2)]/(A_1A_2)$. There is evidence that the bending persistence length increases as salt concentration decreases, plateauing at high salt concentrations (Table 2) [26]. Therefore, the value of 50 nm (above) corresponds to a salt (Na^+) concentration of about 0.15 M. A broader range of torsional-rigidity constants has been suggested in the literature (see [20,27], for example), pointing to a numerical value for C somewhere within the wide range $1.5–4 \times 10^{-19}$ erg cm (or ρ values in the range 0.5 to 1.33). This range corresponds to a twisting persistence length, $p_t = 2C/k_BT$ [28], of 75–200 nm and to an rms twist angle,

$$\langle \theta_t^2 \rangle^{1/2} = \sqrt{\frac{k_BTd}{C}} = \langle \theta_b^2 \rangle^{1/2} \sqrt{\frac{\rho}{2}}, \qquad (1c)$$

in the 3.4–5.5° range. If we use sequence variation measurements of B-DNA crystal structures in the Nucleic Acid Database [2], the mean $\langle \theta_t^2 \rangle^{1/2} = 5.2°$ [19•], which corresponds to $C = 1.66 \times 10^{-19}$ erg cm and $\rho = 1.2$. A lower twist variation, such as observed in solution studies by high-resolution NMR [29], gives rise to higher C and

lower ρ values. Note that as from theory $-1 \leq \sigma_e < 0.5$ [22], we have $0 \leq \rho \leq 1.5$ for homogeneous elastic rods; but considering that no substance is known for which $\sigma_e < 0$, we have the estimate $1 \leq \rho \leq 1.5$. Deviations from the last range are expected for real DNA, a non-uniform material with non-circular cross-sections, where bending is asymmetric (i.e. more rolling than tilting) and twisting is sequence dependent.

In its simplest form, the elastic energy for torsionally stressed DNA modeled as a naturally straight and thin isotropic material can be written as:

$$E = E_B + E_T = \frac{A}{2}\oint \kappa^2(s)ds + \frac{2\pi^2 C}{L_0}(\Delta Lk - Wr)^2, \quad (2)$$

where s denotes the arc length, κ is the curvature, and the integral is evaluated over the contour length of the chain, of length L_0. The topological parameter ΔLk (where Lk is the linking number) describes the torsional stress imposed on the DNA with respect to the value at the relaxed state, Lk_0 (for relaxed DNA, $Lk = Lk_0$ = the number of primary turns = N/h_0, where N is the number of base pairs and h_0 is the helical repeat of the DNA, say 10.5 bp turn^{-1}). The writhing number, Wr, is a geometrical descriptor of DNA shape, roughly the number of times that a DNA molecule crosses itself averaged over all planar projections (for rigorous definitions of all topological and geometrical quantities mentioned above see [30]). The term for the twist energy (E_T) above, reflecting a uniform twist density ω, follows from the assumption of isotropic bending of a thin elastic rod model at equilibrium [14,31••]; the quadratic deviation of the local helical twist from its intrinsic equilibrium value ω_0,

$$(C/2)\oint(\omega - \omega_0)^2 ds,$$

can be expressed in terms of the writhing number Wr and Lk from the topological invariance of $Lk = Tw + Wr$, where the twist

$$Tw = \oint \omega ds \qquad [32].$$

The normalized version of ΔLk, namely the superhelical density $\sigma = \Delta Lk/Lk_0$ is often used to describe torsional stress in DNA systems and is typically around $\sigma = -0.05$ for DNA *in vivo* (except for certain thermophilic bacteria, in which the DNA is positively supercoiled). The symbol σ for superhelical density should not be confused with σ_e, introduced earlier for the Poisson ratio of an elastic material.

For rods that are not naturally straight, the elastic free energy must be modified to model intrinsic (constant) curvature (i.e. non-zero values of κ_0) and a constant torsion, τ_0. Tobias and Olson [31••] show that assuming circular cross-sections, the bending and twisting terms in analogy to Eqn. 2 are given as follows, where θ is the angle between the intrinsic and actual curvature vectors:

$$\hat{E} = \frac{A}{2}\oint(\kappa(s) - \kappa_0)^2 ds + 2A\kappa_0 \oint \kappa \sin^2\frac{\theta}{2} ds + \frac{C}{2}\oint\left(\frac{d\theta}{ds} + \tau - \tau_0\right)^2 ds. \quad (3)$$

Note that in contrast to naturally straight rods the twist energy can no longer be expressed as a constant times $(\Delta Tw)^2$ i.e.,

$$(C/2)\oint(\Delta\omega)^2 ds = \frac{(2\pi^2 C)}{L_0}(\Delta Tw)^2$$

and therefore involves the torsion of the curve, τ, and a derivative of θ. Tobias and Olson [31••] discuss the differences in equilibria between naturally curved and naturally straight materials. In particular, they show that the twist density generally varies with position for rods that are not naturally straight, implying underwound and overwound segments for the DNA with respect to the intrinsic twist density of the molecule. They also suggest that stable solutions, in the form of slightly distorted circles exist for closed intrinsically curved rods.

Analytical advances — entropic effects and new representations

Analytical solutions for the elastic rod based on Kirchhoff's theory provide many useful results on the behavior of DNA under induced torsional stress. Minimization of the mechanical energy under various assumptions of configurational regularity can be achieved by various coordinate-system representations (Euler angle, finite elements, etc.). In order to be relevant to studies of DNA at typical superhelical densities, excluded-volume effects must be taken into account to avoid the unrealistic situation of minimizing the elastic energy by maximizing Wr ($Wr = \Delta Lk$, $E_T = 0$).

The interplay between bend and twist for DNA in the context of elasticity has been explored by many researchers [7•], revealing many interesting properties of DNA, such as the onset of supercoiling [33,34], the abrupt non-planar buckling from the circle to the figure-8 interwound structure, and the expected supercoiled-DNA configurations formed as a function of σ [35,36•]. The tendency of DNA to form interwound configurations (see energy-minimum forms in Fig. 3) rather than toroidal configurations has also been demonstrated on the basis of energetic arguments, in agreement with electron microscopic observations of supercoiled DNA. In this connection, it should be noted that small-angle X-ray scattering (SAXS) profiles also capture global geometric features of superhelical configurations. For example, see Fig. 4 for characteristic SAXS signatures of

a supercoiled DNA molecule at different concentrations of salt.

A recent focus in analytical studies is the consideration of entropic effects and thermal fluctuations on DNA supercoiling. Instead of an excluded-volume term, Lahiri [37•] approximates the configurational entropy (S) term of a supercoiled DNA form by $-T\Delta S = \alpha N/r^2$, where r is the superhelix radius and α is a constant. This analysis applies only to linear, unbranched molecules and ignores pairwise contact among the chain points (though such contact is important for electrostatic considerations). (In this article, the term 'branched' refers only to double-helical DNA branches and not to single-stranded DNA branches, such as those formed by cruciforms.) After simplifying the bending energy in Eqn. 2 on the basis of geometric arguments, Lahiri minimizes the free energy of supercoiling subject to a contour length constraint. This yields many of the relationships among supercoiled DNA parameters that have been observed or obtained by systematic simulation studies. These relationships include

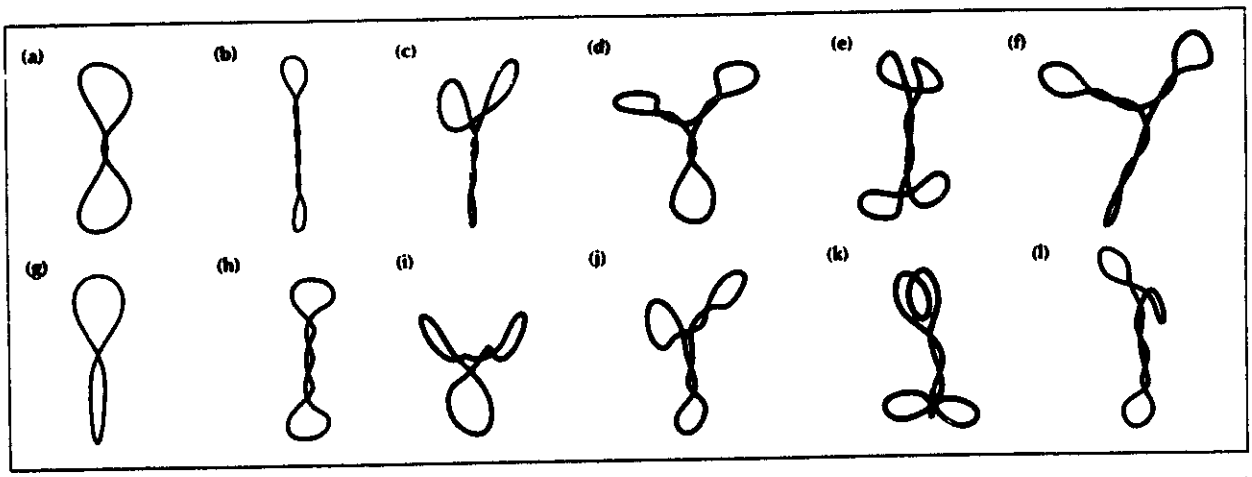

Fig. 3. Energy minimized superhelical DNA forms at sodium salt concentrations of 1.0 and 0.1 M. The energy-minimized structures correspond to bending, twisting, and Debye–Hückel potentials [25•] for a 2000 bp closed circular DNA duplex. The bending constant A is set to the high-salt limit of persistence length (see Table 2 and [25•]), and the torsional-rigidity parameter C is set to reproduce the observed root mean square twist angle of $\langle \theta_t \rangle^{1/2} = 5°$ ($C = 1.8 \times 10^{-19}$ erg cm). Shown in (a–f) are representative 1.0 M minima for: (a) $\Delta Lk = -2$; (b,c) $\Delta Lk = -5$; (d) $\Delta Lk = -8$; (e,f) $\Delta Lk = -10$; with corresponding writhing numbers of −1.67, −4.03, −4.26, −6.29, −7.16, and −7.17. The form shown in (b) is lower in energy than that in (c), and the form shown in (f) is lower in energy than that in (e). The representative 0.1 M minima shown in (g–l) correspond to the same ΔLk associated with (a–f) and have writhing numbers of −1.32, −3.43, −3.85, −4.97, −5.22, and −5.68. Again, the straight interwound form shown in (h) is lower in energy than the Y-shaped interwound shown in (i), and the Y-shaped form shown in (l) is lower in energy than the four-lobed interwound form shown in (k). Note the angular orientations of the end loops of the interwound forms and the much more open, loosely interwound structures formed in the low (0.1 M) salt environment. These data were generated for this review.

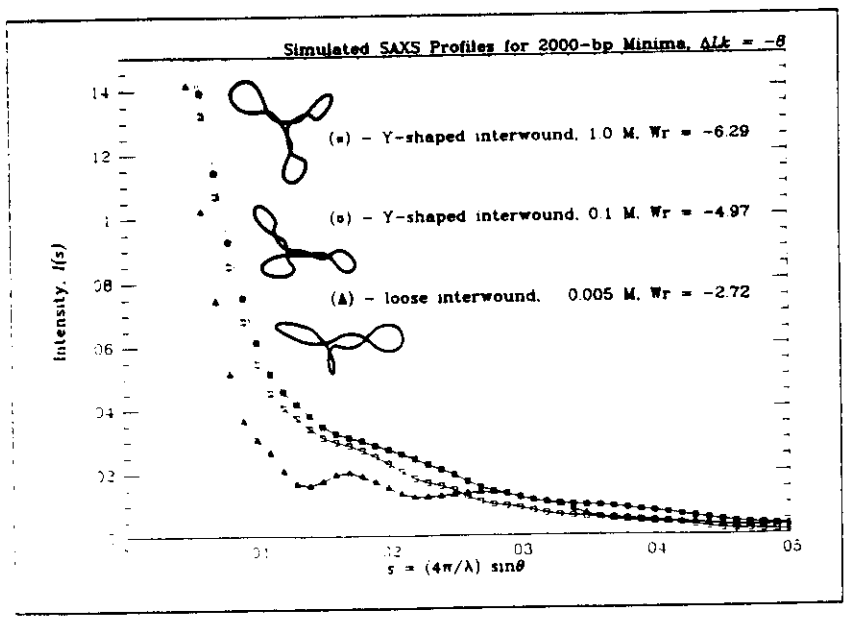

Fig. 4. SAXS Profiles for 2000 bp minima, $\Delta Lk = -8$, at different concentrations of sodium salt. The scattering profiles are computed from the curve coordinates, as shown in Fig. 3, by a discrete form of the Debye integral (for details see [25•]). The profiles reveal a systematic trend in which the DNA supercoils become more loosely coiled as the salt concentration is lowered. This trend was clearly noted in the experimental works of Brady and co-workers [61]. These data were generated for this review.

the direct proportionality of the superhelix axis length to N and that of Wr to ΔLk, as well as the quadratic dependence of the supercoiling energy on ΔLk. In particular, the limiting value for the superhelix radius r is interpreted as resulting from maximization of the entropy of the chain [37•].

Marko and Siggia [38•] similarly focus on how entropy and enthalpy compete to determine supercoil shapes. By applying scaling ideas from polymer statistical mechanics, they express the free energy of supercoiling per unit length as a sum of a Helmholtz free-energy term like Eqn. 2 (A and C are temperature dependent), an entropic penalty term for regular interwound and toroidal superhelices, and a hard-core repulsion term proportional to d^{-12} where d is an interchain separation distance. Thermal motions are considered by assuming Gaussian fluctuations about regular interwound and toroidal superhelices whose pitch, radius, curvature, and average supercoil writhe can be determined explicitly [38•]. By minimizing the resulting energy for a given configurational regime (i.e. interwound, toroidal) with associated pitch and radius, Marko and Siggia show that thermal fluctuations play a critical role in stabilizing the interwound superhelix; as Lahiri also finds, Marko and Siggia note that a radius reduction would suppress fluctuations and therefore cause a loss of entropy. For moderate |σ| the toroidal regime is also shown to be significantly higher in energy than the interwound regime, as expected, but the toroidal form is energetically favorable under special geometric constraints. According to Marko and Siggia, interwound branching — the formation of Y-shaped DNA, as commonly observed in electron micrographs (see also Figs 2,3) — balances entropic costs with enthalpic energy gains.

Shi and Hearst [39••] develop a new, curvature-torsion coordinate framework to study DNA supercoiling on the basis of the non-linear Schrödinger equation. Rather than using the common Euler-angle representation for formulating the differential equations describing the equilibrium of an elastic rod system, their framework focuses on the geometric variables of curvature and torsion, κ(s) and τ(s) (see also discussion in [31••]). They show that the stationary states of supercoiled DNA can be obtained in closed form from the time-independent non-linear Schrödinger equation in one dimension. Self-contact effects can be incorporated through an additional potential. Shi and Hearst study a toroidal helix, solutions for which can be obtained with closed end boundary conditions without consideration of interchain contact. Expressions for Wr and Tw can be explicitly derived. The immediate extension of this novel approach to interwound chains with self contact, to nucleoprotein geometries, and to time-dependent solutions that might suggest local transition pathways associated with gene regulation, for example, promises exciting discoveries.

Buckling transitions: analytical, numerical, and experimental clues

Another interesting analytical study from last year explores the higher-order buckling transitions associated with the elastic rod treatment of DNA [40•]. This work complements two other simulation studies based on numerical energy minimization [36•,41•] and also complements experimental observations. The buckling transition from circle to figure-8 is well known from elasticity theory to depend on $(3)^{1/2}\rho$ (see Fig. 5, computed energy profiles for energy crossing between families F0 and F1 for two ρ values). Interestingly, Zajac [42] first related this result to the coiling and kinking of submarine cables. This buckling catastrophe was later associated with DNA at a threshold $\Delta Lk = (3)^{1/2}\rho$ [33,34], where exchange of stability between the two stable forms occurs. Higher-order transitions had not been analytically demonstrated in this context until last year, though Le Bret [43] has suggested a possible second transition between the figure-8 and the interwound form with a writhe value near two [43].

In an extensive minimization study in 1994 [41•], the existence of the higher-order buckling transitions was demonstrated for a theoretical elastic model with self contact. In this study, a Lennard-Jones term for self contact (both attraction and repulsion) was used, and the elastic plus non-bonded energy was minimized at small |ΔLk| intervals in the range of 0 to 6 for a 1000 bp closed duplex circle. Intriguingly, a notable transition was found between the figure-8 and the next interwound form of Wr ≈ 2 (see Fig. 5a, families F1 and F2) and more subtle jumps in Wr as |σ| was increased (see Wr profiles in Fig. 5a). Each such transition is characterized by a sudden increase in E_B and a sharp decrease in E_T, as well as by a systematic drop in the self-contact term. This behavior was also obtained without attractive forces, and with an explicit Debye–Hückel term instead of the Lennard-Jones potential [25•] (as shown in Fig. 5a,b for two ρ values). With a necessarily simplified self-contact treatment (hard sphere) in the context of finite elements, as configurational families were traversed, sharper drops in E_T were noted than those shown in Fig. 5, accompanied by rises in E_B and Wr [36•]. A close examination of these various profiles, including the most recent Fourier series description by Liu *et al.* [44], suggests that the ratio ρ profoundly affects the nature of the minimization profiles obtained. Note from Fig. 5a, where ρ = 1.5, how much sharper the configurational and energetic variations are with |ΔLk| in comparison with Fig. 5b (ρ = 0.7); the behavior between families F1 and F2 in the Wr curve appears to be particularly sensitive to ρ. A more detailed exploration of this sensitivity to ρ over a broad range is now available (Ramachandran G, Schlick T, unpublished data).

In his study of this phenomenon, Jülicher [40] neglects thermal fluctuations and entropic effects to make

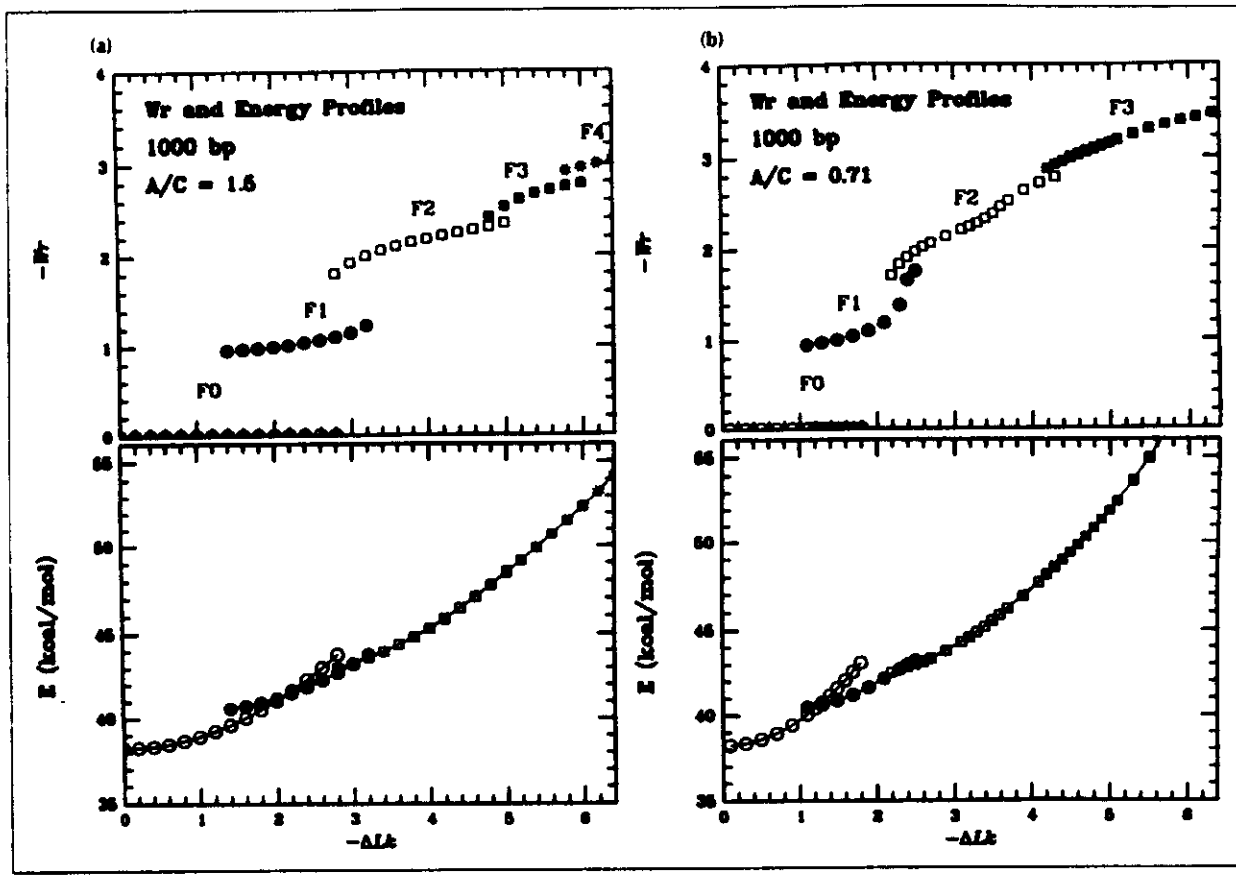

Fig. 5. Configurational profiles for 1000 bp closed duplex DNA as a function of σ for two values of C. The writhe profiles are shown as ΔLk is varied from 0 to −6 for two values of the torsional-rigidity constant C (0.85 and 1.8×10^{-19} erg cm), corresponding approximately to $\langle \theta_t \rangle^{1/2} = 7°$ and 5°, respectively. The energy consists of bending, twisting, and Debye–Hückel components and is set to a sodium salt concentration of 1.0 M, as described in [25•]. For reference, the Coulombic energy for the circle is 37.1 kcal mol^{-1}. Note the existence of more clearly separated families for the lower C (higher ρ) profile. Although only the total energy is shown here, it is easy to distinguish the families on the basis of the twist energy: the beginning of a family is associated with a sharp drop in the twist energy. Note the smoother profile for the larger C (lower ρ) value and the lower ΔLk for the circle→figure-8 buckling at the lower ρ set. The first data set was taken from [25•], and the second was generated for this review. For longer DNA systems, profiles smooth out considerably (G Ramachandran, T Schlick, unpublished data).

his analytical model tractable for solution and exploits the large ratio between length and thickness assumed for the long and thin elastic rod model. Four equilibrium (stationary) families are obtained as solutions of the Euler–Lagrange equations: planar circles ($Wr = 0$), non-planar rings ($0 < Wr \leq 1$), self-intersecting rings ($1 < Wr \leq 2$), and interwounds ($Wr > 2$). Depending on the numerical value of ρ, the transitions between families are discontinuous or continuous. Interestingly, the branch of non-planar rings is unstable for $\rho > 0.61$. (Note that slight deviations from homogeneity of bending or from circular cross-sections can alter the precise value of ρ at which instability occurs.) This branch of non-planar rings is not typically found by numerical minimization procedures. This equilibrium description not only underscores the sensitivity of the results to the elastic parameters and the need for careful selection for numerical models, but also brings into immediate question the biological relevance of these buckling phenomena.

Are these configurational transitions masked by thermal fluctuations in real DNA? This is certainly expected; also, as plasmid size is increased, the Wr and energy profiles (as shown in Fig. 5) are expected to smooth out rapidly (Ramachandran G, Schlick T, unpublished data). Even if so, might these buckling phenomena be relevant under certain situations? The views shown in Fig. 5a,b for two ρ values, taken along with Jülicher's result, clearly demonstrate that the larger the value of ρ, the more abrupt the catastrophes will be. Thus, if A is taken to be fixed, these buckling transitions will be more important for smaller C values. Furthermore, for small duplex circles (e.g. a few hundred base pairs), the transitions of lower order (because physiological σ implies small $|\Delta Lk|$) are expected to be important. More generally, such phenomena may affect structural behavior in small, looped segments of DNA, which act topologically like closed minicircles. Very recently, buckling transitions for 178 bp minicircles *in vitro* have been observed by cryo-electron microscopy [45••]. Furthermore, on the

basis of time-resolved fluorescence polarization and dynamic light-scattering measurements, the laboratory of Schurr [46] reported abrupt structural changes in supercoiled DNA plasmids as physiological superhelical densities are approached (in most studies, only physiological σ is explored). These transitions may involve coupling between secondary and tertiary structure. Interestingly, Schurr and co-workers [27] have also suggested lower C values on the basis of the plasmids studied in their laboratory. This is the case where buckling phenomena might be more significant.

Abrupt structural transitions associated with DNA supercoiling may also play a role in mechanisms guiding protein–DNA complex formation, regulated by proteins that wrap and bend DNA. An interesting analytical study of such structural transitions has been presented by Tobias *et al.* [47•]. Their analysis accounts for, and generalizes, the sudden configurational changes of DNA when wrapped around a protein, as observed by computer simulations [48•]. In the study by Tobias *et al.* [47•], expressions are derived for the equilibrium configurations of long DNA systems subject to a variety of boundary conditions at the DNA ends. The elastic-rod framework of Kirchhoff is used, and explicit solutions are derived in a cylindrical coordinate system using the equilibrium theory of traveling waves. Tobias *et al.* show that small changes in end conditions can result in large changes of three-dimensional structure. For example, nicked DNA (for which explicit formulas for equilibrium configurations of a twist-free rod are more easily derived than for closed circular DNA) undergoes an abrupt transition as a result of a small angular change ($\Delta\alpha$) in the orientation of the tangent vector at one end of the rod with respect to the axial direction of the rod, near a perpendicular orientation ($\alpha = 90°$). Transitions between crossed and open loops are shown to be abrupt as a function of the tangent vector orientation at the boundary, whereas intermediate self-intersecting forms vary continuously. Tobias *et al.* [47•] interpret these observations in terms of a possible correlation between an enzymatic nicking mechanism and the boundary geometry at the DNA ends: depending on the instance of nicking (with respect to the abrupt structural change that takes place), a duplex circle can sustain a ΔLk of one or two. This difference depends on the Wr increment between the time of nicking and ligation, an increment that is shown to depend sensitively on the tangent orientation at the point of contact between the protein and the DNA.

Free energy of supercoiling: experiment and analysis

The issues of entropy (thermal fluctuations) and the relevance of the mechanical elastic equilibria to supercoiled DNA, discussed above, have been further explored by Bauer and Benham [49••]. Experimental data of DNA melting from gel studies in which electrophoretic mobility is regarded to be a function of ΔLk and T (40–60°C) have been analyzed for a DNA plasmid, pBR322 (4361 bp). (The size of this plasmid appears to vary in the literature; the value given here is the most recently reported.), to determine the free energy associated with supercoiling deformations of the DNA and to estimate the enthalpic and entropic contributions to the free energy. Low-salt conditions were used, and the gel data were collected for σ values between −0.058 and +0.02 (the typical density here is −0.054). A quadratic dependence of the supercoiling free energy on ΔLk has been confirmed, and both the entropy and enthalpy of supercoiling are reported to be positive and to vary quadratically with ΔLk. Bauer and Benham suggest that because the estimated magnitude of the entropy term is relatively large (roughly half the magnitude of the enthalpy), enthalpy alone may not reasonably represent the free energy of supercoiling, especially as temperature increases. They argue that the interactions of DNA with its surroundings can be substantial and therefore that caution must be exercised in interpreting simulation work.

Clearly, the data presented by Bauer and Benham in Table I of [49••], regarding best-fit energy parameters for an assumed quadratically varying free-energy expression as a function of σ, form a valuable addition to the literature. The conclusions regarding the total free energy are reasonable and in agreement with other experimental and theoretical studies. It is certainly true that although numerical simulations of DNA supercoiling (such as Monte Carlo methods and MD) account for configurational entropy, they cannot directly model other entropic sources, such as those arising from external interactions between the solute DNA and other molecules. Langevin simulations (see below), however, can model these interactions implicitly through frictional terms and hydrodynamic interactions. Thus, cautionary notes regarding the importance of these additional factors that cannot easily be accounted for via simulation are always timely in the numerical modeling of large and complex biomolecular systems. Nonetheless, two points should be noted. First, the experimentally derived elastic parameters used in simulations reflect in some sense the average behavior of DNA in its natural environment. Second, to date, there is a significant agreement between results obtained with the elastic rod and those obtained with statistical polymer framework. This agreement arises because the simulated configurational properties of supercoiled DNA reflect free-energy contributions to bending and torsional deformations; any direct partitioning into entropy and enthalpy cannot be extrapolated from these results.

Dynamic simulations based on geometric curve representations

As seen above, many interesting aspects of DNA supercoiling can be studied by examining minimum-energy

profiles or 'average' behavior of regular superhelical structures. The floppiness and irregularity inherent in large DNA systems, however, requires that the entire thermally accessible configuration space be considered. Equilibrium distributions as obtained by Monte Carlo simulations form one technique to explore the wide range of spatial configurations and the associated properties of topologically constrained DNA systems. This approach may be classified as statistical, rather than kinetic, in nature. Monte Carlo simulations are straightforward to formulate for supercoiled DNA, efficient to study on modern computers, and valuable for systematically analyzing many observed phenomena related to branching [50], catenation [6], salt effects, etc. Recent adaptations to curved DNA species, for example [51], reveal the strong tendency of an intrinsic bend to be localized at an apex of a superhelix and the dependence of branching patterns (e.g. straight versus Y-shaped forms) on the spatial separation of the bends along the chain.

Nonetheless, procedures that simulate continuous dynamics are essential in order to obtain dynamic information on pathways of structural changes in DNA. Such information is important for understanding configurational transitions in DNA, kinetic processes such as recombination and knotting, and hydrodynamic functions. In recent years, such kinetic views have been offered by molecular, Langevin, and Brownian dynamics formulations in a variety of modeling frameworks. These methods are based on numerical integration of Newton's equations of motion:

$$M\dot{V}(t) = -\nabla E(X(t)), \quad \dot{X}(t) = V(t) \qquad (4)$$

for the collective position and velocity vectors, X and V, as a function of time, t. The symbol M denotes the mass matrix; the dot superscripts represent differentiation with respect to time; and the systematic force is expressed as the negative gradient vector of the potential energy E(X). The different dynamic methods developed for supercoiled DNA have different physical and computational features. These, in turn, influence the topics and systems studied using these methods.

Molecular dynamics

The elegant three points per bp ('3DNA') model of Tan and Harvey [52] forms a compromise between computational feasibility and physical reliability for closed circular duplex DNA. A strong feature of their formulation is the possibility to model specific DNA sequences through selective parameter choices for individual bp tilt, roll, and twist potentials. In particular, different force constants for the terms associated with the tilt and roll angles can be used to model anisotropic bending, though this is yet to be done.

Sprous *et al.* (D Sprous, RK-Z Tan, SC Harvey, personal communication) raise general issues of numerical convergence of thermodynamic properties, which are important in light of the significant thermal fluctuations expected from DNA systems of several thousand base pairs. Tan *et al.* (RK-Z Tan, D Sprous, SC Harvey, personal communication) also present a kinetic study of polymer slithering — the reptant-like motion along the chain — and branching. Specifically, they examine three types of 600 bp circles over 500 ns simulations of standard MD with velocity reassignments and a timestep $\Delta t = 31.26$ fs. They find that homogeneous sequences (the same global helical parameters assigned to each bp) slither predominantly, whereas naturally curved sequences (whose roll, tilt, and twist are bp specific) use slithering only to find favorable arrangements that can accommodate small variations in curvature so that more highly curved regions cluster at the loop tips of branched superhelices. A regular curved sequence (a curved central insert of 50 bp of composition $[A_5G_5]_5$) reveals, in contrast, little variation in the branch geometry, favoring an apex at the center of the inserted curve. These findings agree with results from other simulations as well as with experimental observations. The model presented by Harvey and co-workers can be extended to longer DNA systems of biological interest, limited only by computer time.

Langevin dynamics

The use of dynamic simulations to study DNA supercoiling has also been described by Olson and co-workers [24]. We use a compact B-spline representation for the DNA curve, as in other energy minimization approaches, but apply a new technique for dynamics based on the Langevin formalism. As a first-order approximation, the internal energy of Eqn. 2 is used (in addition to self-contact and chain-length terms); clearly, the assumption of uniform twist at every dynamic step makes solution straightforward, but is unsatisfactory in the long run. The dynamic implementation involves the use of a highly stable numerical integration scheme for the Langevin equation [24], making possible supercoiled DNA simulations entering the microsecond range (timesteps between 0.1–1 ns) [53,54•].

The Langevin formalism has a long history in modeling, originating from the study of liquids and polymers in the 1940s [55,56]. This framework provides a useful body of knowledge for modeling physical systems in viscous media. In addition to a first-order approximation of solvent damping, the Langevin model is computationally efficient, as an optimal coupling of the system to the thermal reservoir accelerates configurational sampling during finite-length simulations [54•]. The Langevin equation includes a frictional term proportional to the velocity and a random force R in addition to the systematic force. In such a way, it crudely mimics molecular collisions and viscosity in the realistic cellular environment. A thermal equilibrium is established through setting the random-

force components (mean and autocovariance matrix below) according to the fluctuation/dissipation theorem:

$$M\dot{V}(t) = -\nabla E(X(t)) - \gamma MV(t) + R(t), \quad (5a)$$

$$\langle R(t)\rangle = 0, \langle R(t)R(t')^T\rangle = 2\gamma k_B TM\delta(t-t'). \quad (5b)$$

In this simplest form of the Langevin equation, γ is the damping constant, and δ is the usual Dirac delta symbol. A more general form of the Langevin equation also includes hydrodynamic effects [56].

In the buckling study discussed above [41•], an analysis of several simulated trajectories of length 1 μs (at effective timesteps of 100 ps [53]) points to four characteristic motions for superhelical DNA (in increasing frequency of timescales): translational diffusion, overall end-over-end tumbling, large-scale bending and twisting about the global helical axis, and local fluctuations in chain curvature. The fluctuation behavior depends on σ and reveals a significant departure from the enthalpic equilibrium structure, especially for moderate $|\sigma|$ (0.0250–0.030), where fluctuations among several preferred regions in Wr (distinct families) are noted. Folding dynamics of the torsionally stressed circle to the interwound form are also readily captured as well as the local superhelical fluctuations (see Fig. 6 for a new illustration on a 2000 bp system).

A recent examination of the effect of salt on DNA flexibility followed the dynamic behavior of 1000 bp duplex circles under physiological $|\sigma|$ (0.05) at environments of c_s =0.005, 0.1, and 1.0 M sodium concentrations [25•]. An explicit Debye–Hückel term was introduced into those calculations in the form:

$$E_c = B(\beta)\iint \frac{e^{-\beta d_{ij}} dl_i dl_j}{d_{ij}}, \quad (6)$$

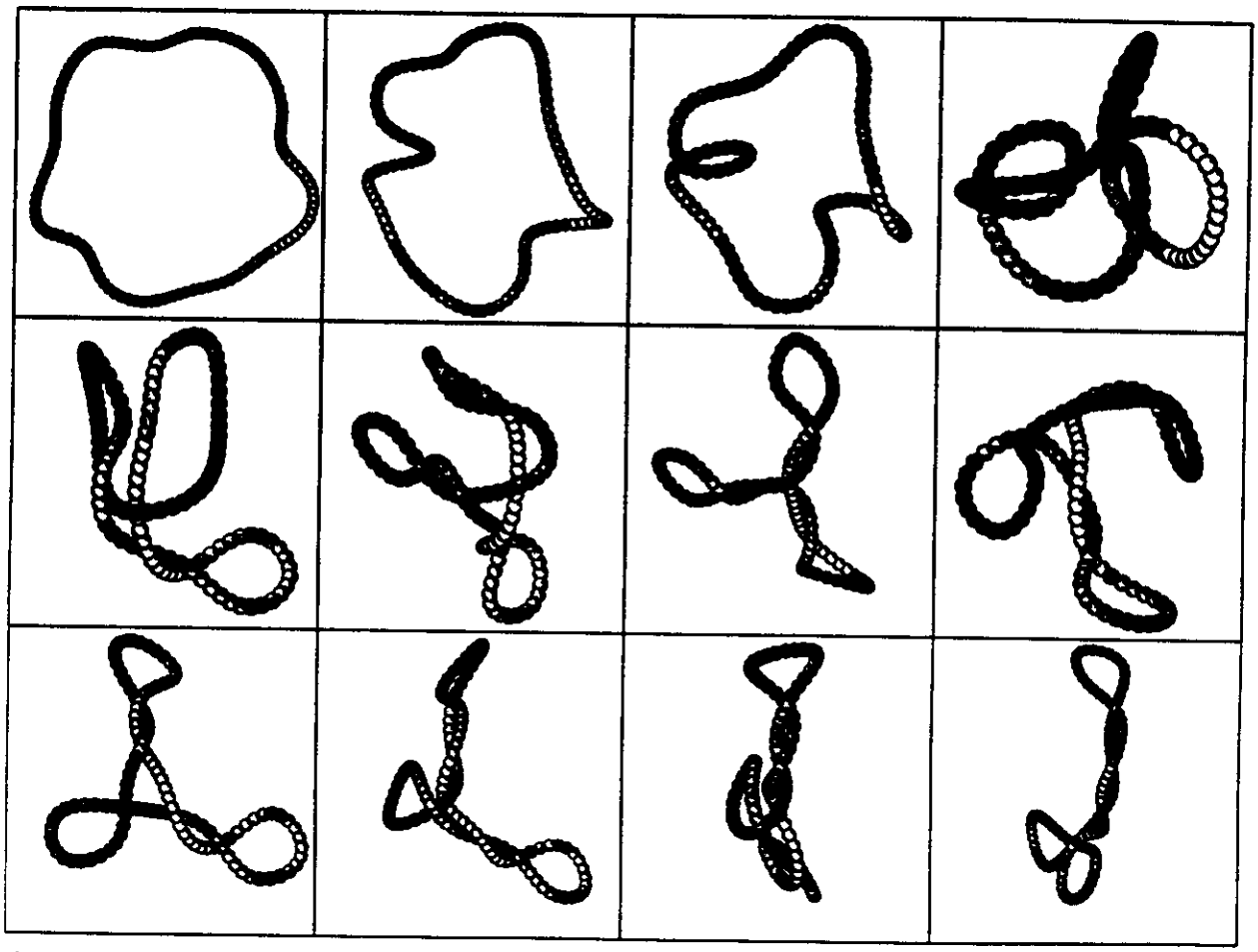

Fig. 6. Branching dynamics of 2000 bp closed duplex DNA. Snapshots of DNA configurations are shown as generated by a Langevin dynamics simulation with moderate solvent damping (as described in [54•]) at $\Delta Lk = -12$ and a salt concentration of 0.1 M. The ratio of the elastic parameters is set to 1, with the bending constant set as described in the legend to Fig. 3. The timestep is approximately one nanosecond, so the total simulation of 10 000 iterations covers 10 μs (six hours of computing on a DEC alpha machine). Note the toroidal-like forms as the DNA begins to fold, followed by branching and formation of lobed-shaped supercoiled structures. Slithering of the DNA segments, as well as global bending and twisting motions, can be observed. Overall, the structures are highly irregular, in contrast to the energy-minimized forms shown in Fig. 3, and reveal the significant opening of the superhelix due to thermal fluctuations and solvent effects. The data were generated for this review, and the visualization was prepared with an interface (written by Constantine Kreatsoulas) between our dynamics programs and the graphics package Molscript [62].

where β is the Debye–Hückel screening parameter ($=0.33\ (c_s)^{1/2}$ at room T), l_i and l_j denote charged DNA segments, d_{ij} is the distance between segments i and j, and B is a salt-dependent coefficient (absorbing both the charge per unit length for the DNA and the dielectric constant of the medium). An interesting pattern emerged from the dynamic simulations: although the DNA forms at low-salt concentrations were loosely supercoiled and more mobile, and those at high salt very compact but rigid, the largest degree of flexibility was noted in the middle range of 0.1 M, near typical physiological values. In this environment there appears to be an optimal balance between electrostatic and entropic factors that makes the DNA overall the most flexible. Furthermore, at this value of salt, a particularly sharp change in the buckling behavior from the circle to the figure-8 was noted (see Fig. 7): as salt concentration decreases below 0.1 M, this transition is delayed sharply (i.e. the critical ΔLk where the energy of the two forms is equal increases from 2.1 to 3.25 as salt decreases from 1.0 to 0.005 M). This finding correlates well with the experimental observations of Bednar *et al.* [45••] , which suggest a sharp 'collapse' of interwound geometries near this critical molarity of salt. The findings also agree with numerical work by Fenley *et al.* [57] involving a more detailed representation of the charged DNA backbone, but on small (100–150 bp) circles.

Most recently, this dynamic model for studying supercoiled DNA has been improved [54•] to treat solvent damping through the viscosity parameter, γ, of the Langevin equation. This addition eliminates harmonic, periodic motion observed earlier in vacuum [24]. In fact, now three regimes of dynamic behavior are identified as a function of solvent damping: at low solvent density (in vacuo behavior), the DNA is globally harmonic, whereas at a high degree of damping inertial forces are small compared to the random collisional forces which dominate DNA's behavior. In the intermediate viscous regime (thought to be characteristic of physiological cellular environments), DNA is highly mobile and active. We suggest that this arises from a critical activation of the global twisting/untwisting mode due to a specific interplay between inertial and diffusive forces. In this regime, transitions among several configurational forms of superhelical DNA are more readily observed, and a preferential lowering of the writhe due to thermal fluctuations is noted. Further, a free energy barrier might exist between two interwound configurations (at the particular ΔLk of the trajectory): the potential energy minimum and a more loosely coiled structure, which is not a potential energy minimum but is an important configuration around which the DNA forms cluster during the dynamic simulation in solvent.

With this first-order solvent representation in the DNA model, a kinetic observation of interwound branching dynamics is possible, as shown in Fig. 6. Quantitative estimates of translational diffusion constants as a function of DNA size are in progress. The relaxation of the

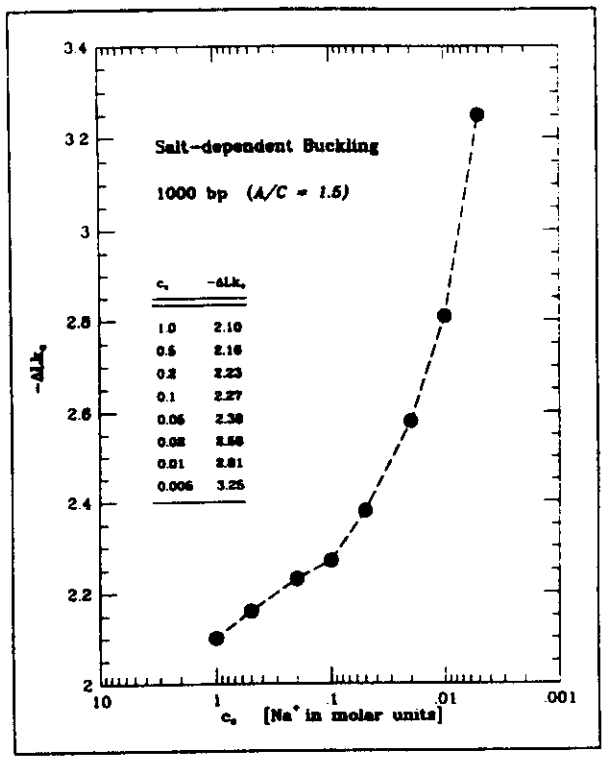

Fig. 7. Buckling of the circle to the figure-8 form as a function of salt concentration. The critical value of $|\Delta Lk|$ where the energy of the circle is equal to the energy of the figure-8 form is shown against the logarithm of the salt concentration. A sharp increase is evident for salt concentrations below 0.1 M. The plotted data are taken from [25•], where $\rho = A/C = 1.5$. With a higher value of C, such as used for Fig. 3, the critical $|\Delta Lk_c|$ shifts downwards consistently, so that at high salt its value is around 1.3 rather than 2.1 (see Fig. 5).

isotropic bending, which implies uniform twist, forms a natural extension of the model. Indeed, the Langevin framework lends itself naturally to other chain representations, such as bead models, where local features reflecting the non-homogeneous bending of DNA can be more easily incorporated than with the compact and global B-spline approach.

Brownian dynamics

When long-time dynamics of systems in solution is of interest, using the Brownian dynamics regime is also reasonable. In this diffusional analog of molecular dynamics, the molecular displacements are considered to be heavily damped by the high viscosity of the solvent. Thus inertial forces are assumed to be small in comparison to solvent damping, so that the motion is overall Brownian (random walk) in character. In this regime, the short-time dynamics behavior is unrealistic, but over long times t, positional displacements of the system satisfy the Einstein relation for the diffusion coefficient D_t as a function of the mean square fluctuations: $6tD_t = \langle |X(t) - X(0)|^2 \rangle$. In practical simulations, the momentum term (velocity term in the right-hand-side

of Eqn. 5a) is neglected, and positions are propagated in terms of systematic and random forces, such as by

$$X(t + \Delta t) = X(t) - \frac{(\Delta t)D_t}{k_B T}\nabla E(X(t)) + R(t) \qquad (7a)$$

$$\langle R(t)\rangle = 0, \langle R(t)R(t + \Delta t)^T\rangle = 2D_t\Delta t\delta_{i,j}, \qquad (7b)$$

in the case of scalar diffusion coefficients and no hydrodynamic interactions. This description can be less realistic than the Langevin formulation of Eqn. 5a,b unless hydrodynamic interactions are included to describe the local force variations due to a change in solvent structure. This description is accomplished by incorporating the local stress variations (i.e. space- and time-dependent diffusion tensor instead of a space- and time-averaged scalar) into the propagation scheme. In practice, the constant D_t is replaced by a matrix whose components depend on molecular positions. This formulation implies interdependence among the components of the random force.

The feasibility of Brownian dynamics techniques to numerical simulations of DNA supercoiling has been reported by Chirico and Langowski [58•]. Their formulation, which relies on Brownian dynamics algorithms developed by McCammon, Garcia de la Torre, Allison, and co-workers (see articles cited in [58•]), uses a bead model to represent closed DNA of 1124 bp (37 bp per bead). Stretching, bending, torsional, and excluded-volume terms are included in the governing potential, and hydrodynamic interactions are included via the Rotne–Prager tensor. The Brownian dynamics protocol follows the motion of the beads (in the framework of three local basis vectors associated with each bead) along with changes in the three Euler rotation angles that orient each bead's axes with the next. In this way, the motion of a 'twisting' ribbon can be followed. In addition to hydrodynamic interactions, non-uniform twist can also be modeled by this approach, making applications to naturally curved sequences feasible.

All parameters typically used in other models require special scaling and adjustment to conform to the bead sizes and the hydrodynamic radii. Although most of these procedures are straightforward, a limitation in this protocol is the use of an elastic deformation energy to describe large angular deviations, such as 40° for non-touching beads. Indeed, kinks are often noted in the generated structures. With a timestep of 95 fs, microsecond simulations are propagated, and the folding of torsionally stressed DNA circles is presented [58•] in agreement with the other dynamic approaches described above. Solvent damping, in particular, leads to significant damping of the globally harmonic modes (expected in vacuum), as also shown recently with the Langevin formalism [54•]. Extensions of the simulation protocol to larger systems is limited by computer time: the computing time grows faster than with the fourth power of the number of beads. In addition, because the diffusive regime averages out the more rapid motions which depend sensitively on the internal potential (such as local changes in curvature), these processes may be poorly resolved or missed by the Brownian dynamics protocol.

Dynamic simulations as extensions of elastic rod theory

In addition to the above dynamic procedures that combine a simplified geometric representation of the DNA with a numerical simulation procedure based on a simplified energy function, dynamic theories of elastic rods can also provide simulation frameworks for supercoiled DNA applications. Indeed, the study of both the statics and dynamics of elastic rods is an active area of research in the field of mechanics. Very recently, the dynamic theory of elastic rods has also been developed to provide numerical simulation frameworks for the evolution in time of a linear elastic rod subject to homogeneous forces (see below). This model is appropriate for a variety of mechanical and biological applications.

Klapper and Tabor (personal communication) describe a new numerical algorithm for the dynamic evolution of the three-dimensional Kirchhoff elastic rod. In their model, the Newtonian equations of motion are formulated for the evolution of a space curve $X(s,t)$ and a twist function $\omega(s,t)$. To express the time evolution of this system, conservation laws for the local forces and torques are formulated and expressed in terms of the curve vector and its tangent, internal and external forces (the latter used to model self contact), and internal (elastic energy) and external (e.g. torsion inertia and damping) moments. To complete the description, the terms are cast in a form ensuring preservation of the total

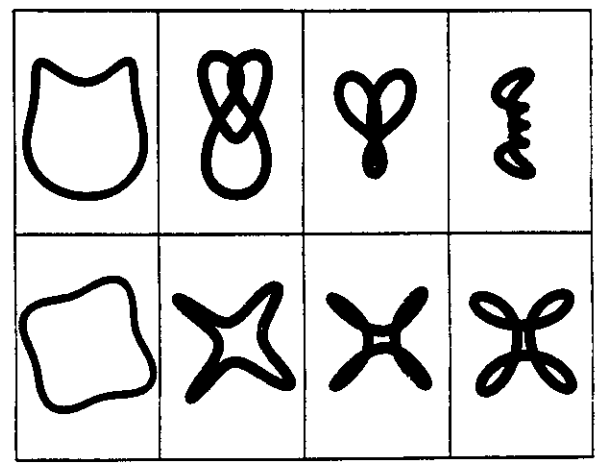

Fig. 8. The dynamic approach to equilibrium forms using simulations of twisted elastic rods. The images displayed were provided by I Klapper. The 'snapshots' shown on top and bottom are taken from two distinct simulations, both with the circular configuration as the initial structure, but with different initial-twist distributions.

contour length. The numerical integration algorithms used are second- and fourth-order explicit (Verlet and Runge–Kutta) schemes, implemented with monitoring of energy conservation and of ΔLk, where appropriate. Boundary conditions can be varied to model both closed and open rods.

Klapper and Tabor obtain illustrative results relevant to DNA supercoiling for the case of closed rods (personal communication). They follow Zajac's instability of the circle→figure-8 transition (no self contact), as well as the folding of two torsionally stressed systems (with self contact in the form of a d^{-10} term) (see Fig. 8). The authors also describe an interesting application for future work involving chain aggregates of bacteria that exhibit complex writhing and buckling phenomena that may depend on the viscosity of the medium.

Similar developments of the dynamics of elastic rods are also in progress by Maddocks and co-workers [59•]. These researchers are formulating the static and dynamic solutions of the elastic rod through numerical quadrature of boundary-value problems of ordinary differential equations for a governing Hamiltonian system.

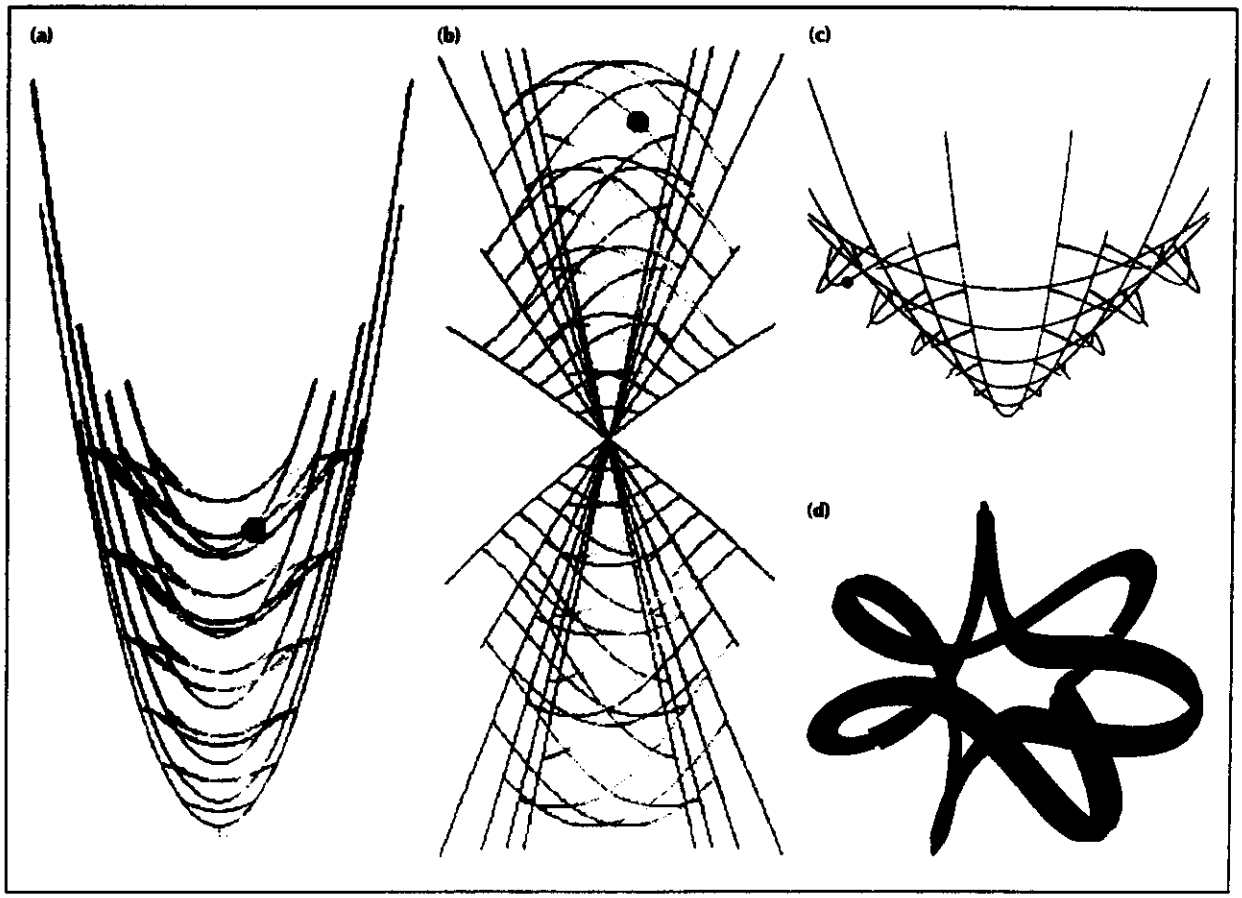

Fig. 9. Representations of the set of equilibrium solutions for an elastic rod model as computed by the programs of Maddocks and co-workers. The results shown here illustrate a sophisticated computational and graphical interactive interface developed by Maddocks and co-workers at the University of Maryland that allows users to visualize the set of equilibrium solutions in an appropriate parameter space and to connect points on the diagram with physical images (equilibrium shapes of the rod [59•]) at selected parameter values. The computations involve solution of a system of ordinary differential equations with boundary conditions that describe the equilibrium shapes of a rod [59•]. The data shown here are for the case of a uniform rod with circular cross-section and no self-contact terms. Other cases can be examined electronically by browsing through the World Wide Web (WWW) site http://jacobi.umd.edu/. Equilibria of the twisted ring problem can be described as one-dimensional (parameter) families when an input variable, such as ΔLk, is varied from a known solution (e.g. the circular configuration). (**a–c**) Three projections, with the ordinate and abscissa as listed, of the bifurcation diagram that arises when the energy, shear force, twist, and writhe are evaluated along these families of equilibria (for mechanical terminology, see [59•]). In each case, the curve is colored (using a spectrum of purple-blue, blue, green, yellow, orange, and red) according to writhe, with green representing Wr = 0 and the upper (red) and lower (blue) limits corresponding to Wr = ±35.5. For this example, certain closed-form solutions are known, namely equilibria in which the axis of the rod assumes a circular shape with either positive or negative twist. These 'trivial' solutions correspond to the straight branches in panel (b) and to the parabolic branches in projections (a) and (c). The other solution branches correspond to configurations in which the axis of the rod is a non-planar curve. The non-trivial branches bifurcate from and link the trivial planar solutions. Panel (**d**) shows the reconstructed physical configuration corresponding to the point indicated by the filled circle in the bifurcation diagrams of panels (a–c). Note that it is knotted, as self-contact is not penalized. The green cylinder represents the center line of the configuration, and the blue ribbon follows the twist of the rod.

Their model can also incorporate self contact and encompasses non-uniform and anisotropic rods that are naturally curved. Equilibrium phase diagrams for the elastic rod are beautifully displayed via an advanced graphics interface that is coupled to computation of the solutions in real time (see Fig. 9 for an illustration). Dynamic extensions are underway.

Conclusions

This review covered selected aspects of recent analytical and kinetic studies in the area of DNA supercoiling. It is already evident from these studies that different scientific communities have been attracted to the world of DNA supercoiling and have brought many diverse and powerful tools. These tools originate from a range of fields, as well as from unusual combinations, such as elasticity theory and Hamiltonian systems, molecular biology and macromolecular simulations, statistical mechanics and polymer theory. The new mathematical rigor by which the functionally important, compactly folded form of DNA is investigated is sharpening many facets of DNA supercoiling and directing attention to the local heterogeneity of the DNA, such as naturally curved sequences and anisotropic bending.

In particular, the profound effects of salt and thermal fluctuations on superhelical DNA structure and dynamics are emerging. Both experiments and simulations are suggesting that kinetic studies, in particular, require a more sensitive treatment for the long-range intrachain interactions than the hard-core approximation that was used for a long time. Furthermore, to understand the configurational flexibility of supercoiled DNA, special attention to the degree of configurational sampling in these numerical simulations is required. Although most of the salt-effect modeling studies have been restricted to univalent ions (sodium), the more complex effects of larger ions and high ionic strengths on the DNA polyelectrolyte require further investigation. Studies are needed to better understand observations regarding substantial compression of the interwound superhelix at high-salt conditions, and novel packing schemes of duplex DNA crystal structures when bound to magnesium. Special attractive terms may be necessary to reproduce experimental trends in this connection.

An important interplay between theory and experiment is also arising. New analytical treatments (e.g. modern Kirchhoff rod theory) are suggesting subtle structural trends (e.g. buckling of rods) that are spurring simulation studies; these, in turn, are leading to a search for biological examples where the detected phenomena may be relevant (e.g. DNA loops, minicircles, DNA–protein interactions). Conversely, experimental data (e.g. observations of salt-dependent DNA knotting and flexibility) are inviting comprehensive and systematic modeling studies to isolate the essential features that best explain, and go beyond, the data.

Of particular interest in the coming years will be new developments in dynamic simulations based on elastic rod theory, kinetic aspects of superhelical DNA as explored by Langevin and molecular dynamics simulations for non-uniform twist and heterogeneous-sequence cases, and advances in experimental techniques to resolve local aspects of DNA structure. Natural extensions of these studies will involve protein–DNA interactions, especially phenomena related to topological constraints, such as in nucleoprotein complexes. Ultimately, two related topics that will require attention are the effects of DNA crowding in the natural cellular environment, and differences in the noted behavior of supercoiled DNA (e.g. in reference to salt effects, see [25•]) between *in vitro* and *in vivo* conditions.

Acknowledgements

I am grateful to Bill Bauer, Craig Benham, David Beveridge, Nick Cozzarelli, Steve Harvey, John Hearst, Maxim Frank-Kamenetskii, Isaac Klapper, Steve Levene, John Maddocks, Wilma Olson, Ned Seeman, Irwin Tobias, and Alex Vologodskii for valuable discussions and/or for sharing their recent works. I thank Gomathi Ramachandran for kindly providing the data for Fig. 5b and for preparing Fig. 6. I am indebted to the support of the National Science Foundation (CHE-9002146, Presidential Young Investigator Award ASC-9157582, and Grand Challenge Award ASC-9318159, the last mentioned co-funded by Advanced Research Projects Agency), the National Institutes of Health (Parallel Computing Resource for Structural Biology award RR08102), and the Alfred P Sloan Foundation. I am an investigator of the Howard Hughes Medical Institute.

References and recommended reading

Papers of particular interest, published within the annual period of review, have been highlighted as:

- • of special interest
- •• of outstanding interest

1. Sarma RH, Sarma MH (Eds): *Structural biology: the state of the art. Proceedings of the Eighth Conversation in the Discipline Biomolecular Stereodynamics, vols 1,2: 1993 June 22–26; Albany.* Schenectady: Adenine Press: 1994.

•• These volumes contain a large collection of studies presented at the June 1993 Biomolecular Stereodynamics meeting at the State University of New York at Albany. Topics include DNA–protein interactions, chromatin structure, transcription, DNA supercoiling, peptide nucleic acids, RNA structure, DNA triplexes and quadruplexes, DNA hydration, and DNA bending.

2. Berman HM, Olson WK, Beveridge DL, Westbrook J, Gelbin A, Demeny T, Hsieh S-H, Srinivasan AR, Schneider B: **The nucleic acid database: a comprehensive relational database of three-dimensional structures of nucleic acids.** *Biophys J* 1992, 63:751–759.

3. Beveridge DL, Ravishanker G: **Molecular dynamics studies of DNA.** *Curr Opin Struct Biol* 1994, 4:246–255.

• An overview of MD studies of DNA (on the all-atom level) is given, with the emphasis on quantitative comparisons of the results of MD studies

with the results of crystallographic and NMR studies. Also examined are *in vacuo* versus *in aquo* simulations as well as modeling issues, such as the treatment of long-range non-bonded interactions.

4. • Bustamate C, Erie DA, Keller D: **Biochemical and structural applications of scanning force microscopy.** *Curr Opin Struct Biol* 1994, 4:750–760.

A summary of progress in SFM imaging of biological systems is presented, including new structural results (e.g. of Cro–DNA complexes) using standard contact imaging, new technical advances, and the use of SFM as a non-imaging tool to record structural changes in space and time associated with molecular function.

5. • Malhotra A, Gabb HA, Harvey SC: **Modeling large nucleic acids.** *Curr Opin Struct Biol* 1993, 3:241–246.

Novel algorithms to model large RNA and DNA systems are reviewed. These models are based on compact representations (i.e. large reduction of the number of degrees of freedom), such as helicoidal coordinates, simplified energy functions (e.g. elastic models), and efficient conformational-search tools. Topics mentioned in connection with closed circular DNA are finite element analyses, energy minimization algorithms, and Monte Carlo and molecular dynamics simulations.

6. Vologodskii AV, Cozzarelli NR: **Supercoiling, knotting, looping, and other large-scale conformational properties of DNA.** *Curr Opin Struct Biol* 1994, 4:372–375.

7. • Vologodskii AV, Cozzarelli NR: **Conformational and thermodynamic properties of supercoiled DNA.** *Annu Rev Biophys Biomol Struct* 1994, 23:609–643.

Experimental and theoretical advances in the study of DNA supercoiling since the 1960s are summarized. The authors survey in particular results obtained to date by Metropolis/Monte Carlo simulations, relating to DNA structure as a function of ionic strength, chain length, and superhelical density; trends of DNA branching; and the thermodynamics of supercoiling.

8. Levene SD: **Conformation and energetics of supercoiled DNA: experimental and theoretical studies.** In *Nucleic acids and molecular biology*, vol 8. Edited by Eckstein F, Lilley DMJ. Berlin: Springer-Verlag; 1994:119–132.

9. Saenger W: *Principles of nucleic acid structure*. Springer Advanced Texts in Chemistry. New York: Springer-Verlag; 1984.

10. Cozzarelli NR, Wang JC (Eds): *DNA topology and its biological effects*. Cold Spring Harbor: Cold Spring Harbor Laboratory Press; 1990.

11. Bates AD, Maxwell A: **DNA topology.** New York: Oxford University Press; 1993.

12. •• Sinden RR: *DNA structure and function*. San Diego: Academic Press; 1994.

This clear and nicely illustrated textbook on DNA structure focuses on the wide variety of known conformations of DNA in addition to the right-handed double helix as first described by Watson and Crick. Topics include DNA supercoiling and bending, experimental techniques for DNA study, cruciform formation, Z-DNA forms, intramolecular triplexes, protein–DNA complexes, and chromosomal organization.

13. •• Frank-Kamenetskii MD: *Unravelling DNA*. New York: VCH Publishers; 1993.

This book, translated from Russian by L Liapin, is a lively and highly entertaining tale of the fundamental material of heredity, the DNA molecule. In the style of a gripping detective novel, the author describes the rise of molecular biology beginning from the physics groundwork of the 1930s. He then describes important biological questions related to DNA (including supercoiling, knotting, and unusual forms) and moves on to discuss many important modern topics including genetic engineering, DNA and disease, and applications of molecular biology to drug design.

14. Fuller FB: **The writhing number of a space curve.** *Proc Natl Acad Sci USA* 1971 68:815–819.

15. Fuller FB: **Decomposition of the linking number of a closed ribbon: a problem from molecular biology.** *Proc Natl Acad Sci USA* 1978, 75:3557–3561.

16. Zhurkin VB, Lysov LP, Ivanov V: **Anisotropic flexibility of DNA and the nucleosomal structure.** *Nucleic Acids Res* 1979, 6:1081–1096.

17. Schellman JA: **The flexibility of DNA. I. Thermal fluctuations.** *Biophys Chem* 1980, 11:321–328.

18. •• Olson WK, Babcock MS, Gorin A, Liu G-H, Markey NL, Martino JA, Pedersen SC, Srinivasan AR, Tobias I, Westcott TP, Zhang P: **Flexing and folding of double helical DNA.** *Biol Chem* 1995, *in press*.

A summary of the excellent work related to long DNA performed in Olson's laboratory last year, covering spatially constrained DNA, Fourier series representation of DNA, and protein-induced effects on DNA structure.

19. • Gorin AA, Zhurkin VB, Olson WK: **B-DNA twisting correlates with base pair morphology.** *J Mol Biol* 1995, in press.

A twist-clash correlation is introduced to account for the sequence-dependent twisting and bending of individual base pairs observed in B-DNA crystal structures. Such relationships are discussed in terms of the effects of primary chemical sequence on the intrinsic global folding of the unconstrained open double helix.

20. Hagerman PJ: **Flexibility of DNA.** *Annu Rev Biophys Biophys Chem* 1988, 17:265–286.

21. Schellman JA: **Flexibility of DNA.** *Biopolymers* 1974, 13:217–226.

22. Landau LD, Lifshitz EM: *Course of theoretical physics: theory of elasticity*, vol 7, edn 3. Elmsford: Pergamon Press; 1986.

23. Hao M-H, Olson WK: **Global equilibrium configurations of supercoiled DNA.** *Macromolecules* 1989, 22:3292–3303.

24. Schlick T, Olson WK: **Supercoiled DNA energetics and dynamics by computer simulation.** *J Mol Biol* 1992, 223:1089–1119.

25. • Schlick T, Li B, Olson WK: **The influence of salt on DNA energetics and dynamics.** *Biophys J* 1994, 67:2146–2166.

A detailed computational study examines the influence of salt (modeled through a Debye–Hückel potential) on the configurations, energies, and dynamics of supercoiled DNA. Dramatic variations in equilibrium shapes and associated dynamics as a function of sodium concentration (0.005–1.0 M) are reported: highly compact and bent interwound states at high salt that are fairly rigid versus much more open and loosely interwound supercoils at low salt that are highly dynamic, with dominant electrostatics and notable slithering. The buckling transition between the circle and figure-8 forms is delayed as salt concentration decreases, with a particularly sharp increase in ΔLk below 0.1 M. A new family of three-lobed, branched supercoiled DNA configurations is also presented, becoming branched interwounds for long chains as ΔLk increases. By simulating small-angle X-ray scattering (SAXS) profiles for the optimized configurations, it is shown that the open, loose supercoils at low-salt concentrations yield consistent patterns with SAXS experiments, therefore offering a new interpretation to the data: a change from closed to open forms as salt level is decreased, rather than a change from interwound to toroidal forms.

26. Manning GS: **A procedure for extracting persistence lengths from light-scattering data on intermediate molecular weight DNA.** *Biopolymers* 1981, 20:1751–1755.

27. Schurr JM, Fujimoto BS, Wu P, Wu P, Song L: **Fluoresence studies of nucleic acids: dynamics, rigidities, and structures.** In *Topics in fluoresence spectroscopy*, vol 3. *Biochemical applications*. New York: Plenum Press; 1992.

28. Manning GS: **Three persistence lengths for a stiff polymer with an application to DNA B-Z junctions.** *Biopolymers* 1988, 27:1529–1542.

29. Ulyanov NB, James TL: **Statistical analysis of DNA duplex structures in solution derived by high resolution NMR.** *Appl Magn Reson* 1994, 7:21–42.

30. White JH: **An introduction to the geometry and topology of DNA structures.** In *Mathematical methods for DNA sequences*. Edited by Waterman MS. Boca Raton: CRC Press; 1989:225–253.

31. •• Tobias I, Olson WK: **The effect of intrinsic curvature on supercoiling — predictions of elasticity theory.** *Biopolymers* 1993, 33:639–646.

Elementary first-order elasticity theory is developed for naturally curved elastic rods, and the consequences of natural curvature in DNA on equilibrium structures are discussed. Results differ, as expected, from the case of naturally straight rods. The torsion of an open segment with a curved

duplex axis can vary with the temperature and the intrinsic twist. In turn, an imposed helicity, such as that associated with binding to proteins, can change the intrinsic twist. The twist density, furthermore, is generally position dependent for naturally curved elastic materials.

32. White JH: **Self-linking and the Gauss integral in higher dimensions.** *Am J Math* 1969, 91:693–728.

33. Le Bret M: **Catastrophic variation of twist and writhing of circular DNAs with constraint?** *Biopolymers* 1979, 18:1709–1725.

34. Benham CJ: **Onset of writhing in circular elastic polymers.** *Phys Rev A* 1989, 39:2852–2856.

35. Hearst JE, Hunt NG: **Statistical mechanical theory for the plectonemic DNA supercoil.** *J Chem Phys* 1991, 95:9322–9327.

36. • Yang Y, Tobias I, Olson WK: **Finite element analysis of DNA supercoiling.** *J Chem Phys* 1993, 98:1673–1686.
A rigorous presentation is given for the adaptation of a finite-element approach to the study of DNA supercoiling. The formulation treats self-contact in a simplified manner and can be used to find equilibrium configurations and associated elastic energies as a function of ΔLk on the basis of Kirchhoff's rod theory. Resulting interwound structures are presented, and are in agreement with analytical and theoretical studies. In particular, the Wr versus ΔLk profile reveals distinct configurational families, with states of odd integral Wr values associated with very small twist energies. Extensions of the model to non-circular cross sections, heterogeneous bending, and curved sequences are discussed.

37. • Lahiri A: **Structure and energetics of plectonemically supercoiled DNA.** *Biopolymers* 1994, 34:799–804.
An analytical study of supercoiled DNA equilibria is presented to examine the relationships among supercoiled DNA variables, namely the number of base pairs, Wr, ΔLk, superhelix radius, superhelix axis length, and the free energy of supercoiling. The standard excluded-volume term is replaced by an entropic term based on a simple geometric estimate. Minimization of the supercoiling free-energy function yields various structural relationships that have been observed experimentally and numerically.

38. • Marko JF, Siggia ED: **Fluctuations and supercoiling of DNA.** *Science* 1994, 265:506–508.
Supercoiled DNA equilibria are examined analytically on the basis of polymer statistical mechanics. Thermal fluctuations, in particular, are accounted for through consideration of Gaussian fluctuations of polymer chains. The supercoil radius and pitch resulting from a competition of entropic and elastic components are discussed, as well as the extension of supercoiled DNA by an applied force.

39. •• Shi Y, Hearst JE: **The Kirchhoff elastic rod, the nonlinear Schrodinger equation, and DNA supercoiling.** *J Chem Phys* 1994, 101:5186–5200.
A new analytical framework is presented for studying equilibria and (by extension) dynamic processes, of DNA supercoiling. The treatment is based on a geometric, torsion-curvature representation and solution of a partial differential equation (the Schrödinger equation). Self contact can be included in the guiding energy function. Results are described for the toroidal stationary states, for which Wr and Tw can be obtained, and extensions to the interwound regime and time-dependent solutions are mentioned.

40. • Jülicher F: **Supercoiling transitions of closed DNA.** *Phys Rev E* 1994, 49:2429–2435.
Conformational transitions for supercoiled DNA are described on the basis of equilibrium profiles of an elastic energy function for a homogeneous rod with a large length:thickness ratio. Only steric self-avoidance of the rod is considered. Complex phase diagrams are obtained for ΔLk in the range of 0–3 and the bending:twisting ratio of the elastic constants, A/C, in the range 0.4–3.3. The generated patterns of configurational families show the sensitivity of the nature of phase transitions (continuity or discontinuity) to the numerical value of A/C. In particular, the family of non-planar circles is stable only at sufficiently low values of A/C.

41. • Schlick T, Olson WK, Westcott T, Greenberg JP: **On higher buckling transitions in supercoiled DNA.** *Biopolymers* 1994, 34:565–598.
A combination of detailed energy minimization and dynamic simulations reveals higher-order buckling catastrophes in supercoiled DNA in the elastic-rod framework. These phenomena may be of particular importance to short DNA chains, DNA loops, and/or topologically constrained DNA at low superhelical densities. The different families identified include the circle, the figure-8, an interwound form with Wr = 2, and more highly interwound structures, which merge at large |ΔLk|. The beginning of each configurational family is associated with a drop in twist energy and a rise in bending energy, a pattern particularly pronounced for the circle→figure-8 and the figure-8→Wr = 2 interwound transitions. These trends might be related to observed changes in DNA structure reported in time-resolved fluorescence polarization and dynamic light scattering measurements of DNA plasmids at increasing σ. The dynamic studies follow transitions among the families, relate mobility to σ, and identify several characteristic motions, including macroscopic bending and twisting about the global helical axis, end-over-end tumbling, and local bending variations.

42. Zajac EE: **Stability of two planar loop elasticas.** *Trans ASME J Appl Mech* 1962, 29:136–142.

43. Le Bret M: **Twist and writhing in short circular DNAs according to first-order elasticity.** *Biopolymers* 1984, 23:1835–1867.

44. Liu G, Olson WK, Schlick T: **Application of Fourier analysis to computer simulation of supercoiled DNA conformation.** *Comp Polymer Sci* 1995, in press.

45. •• Bednar J, Furrer P, Stasiak A, Dubochet J, Egelman EH, Bates AD: **The twist, writhe and overall shape of supercoiled DNA change during counterion-induced transition from loosely to a tightly interwound superhelix. Possible implications for DNA structure *in vivo*.** *J Mol Biol* 1994, 235:825–847.
A cryo-electron microscopy study, along with analyses by Metropolis/Monte Carlo simulations, is presented to examine the effects of salt repulsion on the structure of supercoiled DNA. It is shown that high ionic concentrations lead to a higher fraction of ΔLk to be partitioned into writhe. In these tightly interwound DNA supercoils, the opposing end segments appear to be in contact with each other. This geometry is postulated to be an important functional state of the DNA. A sharp structural transition is also reported for 178 bp minicircles at ΔLk = −2 as salt concentration is increased. The Monte Carlo simulations provide a further tool to analyze the observed trends and show generally good agreement with experiment, except for notable discrepancies at high concentrations of salt, possibly due to both the polygonal representation of the DNA and the stiff non-bonded potential used.

46. Song L, Fujimoto BS, Wu P, Thomas JC, Shibata JH, Schurr JM: **Evidence for allosteric transitions in secondary structure induced by superhelical stress.** *J Mol Biol* 1990, 241:307–326.

47. • Tobias I, Coleman B, Olson WK: **Dependence of DNA tertiary structure on end conditions: theory and implications for topological transitions.** *J Chem Phys* 1994, 101:10990–10996.
An analytical study of abrupt structural transitions that may be associated with DNA bending proteins is performed by deriving equilibrium configurations of long DNA systems modeled as elastic rods, subject to different boundary conditions at the ends (where proteins bind to the DNA). It is shown that small changes in the orientation of the tangent vector can lead to abrupt changes in three-dimensional structure. These results are interpreted in terms of an enzymatic nicking/ligation mechanism that changes the linking number of closed DNA loops. See also [48•].

48. • Zhang P, Tobias I, Olson WK: **Computer simulation of protein-induced structural changes in closed circular DNA.** *J Mol Biol* 1994, 242:271–290.
Computer simulations using a Fourier series representation of the DNA and Metropolis/Monte Carlo simulations for energy minimization are used to study the configurational properties of closed circular DNA bound to proteins. A modeling scheme is introduced to describe configurations of closed circular DNA, segments of which are wrapped around a core of proteins. The energy includes bending, twisting, and excluded-volume terms. By varying the geometries of the wrapped segments, the number of superhelical turns, chain length, and imposed ΔLk, the authors observe a sudden change in tertiary structure of the double helix in response to altered wrapping of the DNA about protein structures. This behavior is analyzed in the context of the 'linking number paradox' associated with nucleosome formation. [47•] presents the analytical theory to account for these observations.

49. •• Bauer WR, Benham CJ: **The free energy, enthalpy, and entropy of native and of partially denatured closed circular DNA.** *J Mol Biol* 1993, 234:1184–1196.
This study combines numerical analysis with gel electrophoresis of early melting of DNA in circular pBR322 DNA to examine the free energy of supercoiling, specifically the relationship between the entropy and enthalpy. It shows that both the entropy and enthalpy vary quadratically with ΔLk and are positive, with the magnitude of the enthalpic compo-

nent approximately double the size of the entropic term. A table is given for best-fit energy parameters for free-energy expressions as a function of temperature.

50. Vologodskii AV, Levene SD, Klenin KV, Frank-Kamenetskii MD, Cozzarelli NR: **Conformational and thermodynamic properties of supercoiled DNA.** *J Mol Biol* 1992, 227:1224–1243.

51. Klenin KV, Frank-Kamenetskii MD, Langowski J: **Modulation of intramolecular interactions in superhelical DNA by curved sequences: a Monte-Carlo simulation study.** *Biophys J* 1995, 68:81–88.

52. Tan RK-Z, Harvey SC: **Molecular mechanics model of supercoiled DNA.** *J Mol Biol* 1989, 205:573–591.

53. Schlick T, Li B, Hao M-H: **Calibration of the timestep for molecular dynamics of supercoiled DNA modeled by B-splines.** In *Structural biology: the state of the art. Proceedings of the eighth conversation in the discipline of biomolecular stereodynamics, vol I: 1993 June; Albany.* Edited by Sarma RH, Sarma MH. Schenectady: Adenine Press; 1994:157–174.

54. • Ramachandran G, Schlick T: **Solvent effects on supercoiled DNA dynamics explored by Langevin dynamics simulations.** *Phys Rev E* 1995, in press.

A kinetic study by Langevin dynamics is presented on the effects of solvent on the dynamics of supercoiled DNA. Three physical regimes of viscosity (or solvent density) are identified: low viscosity, characterized by globally harmonic motion; intermediate viscosity, associated with high mobility and maximal sampling; and high viscosity, reflecting extreme damping of all global DNA modes. It is suggested that in the intermediate solvent range, a critical activation of the twisting/untwisting mode accelerates configurational transitions between tightly interwound structures and more loosely coiled forms, favored because of thermal fluctuations.

55. McQuarrie DA: *Statistical mechanics.* New York: Harper Row; 1976:chapters 20 and 21.

56. Berne BJ, Pecora R: *Dynamic light scattering: with applications to chemistry, biology, and physics.* New York: Wiley; 1976.

57. Fenley MO, Olson WK, Tobias I, Manning GS: **Electrostatic effects in short superhelical DNA.** *Biophys Chem* 1994, 50:255–271.

58. • Chirico G, Langowski J: **Kinetics of DNA supercoiling studied by Brownian dynamics simulation.** *Biopolymers* 1994, 34:415–433.

A Brownian dynamics simulation procedure for supercoiled DNA is presented, with illustrative results for the relaxation of a torsionally stressed 1124 bp plasmid from the circular to the interwound form.

59. • Dichmann DJ, Li Y, Maddocks JH: **Hamiltonian formulations and symmetries in rod mechanics.** In *Proceedings of the Institute for Mathematics and its Applications program in mathematical biology: IMA volumes in mathematics and its applications.* Edited by Sumners DW. New York: Springer-Verlag; 1995, in press.

A survey of contemporary rod mechanics is presented, including both dynamics and statics. The majority of the exposition is classic material within the mechanics community, but provides a nicely self-contained account for DNA modelers. Several results and computations obtained by the authors are also described, with emphasis on the role that Hamiltonian formulations and symmetries play in efficient numerics, special solutions, conservation laws of dynamics, and integrals of statics. The models described incorporate self-contact effects and encompass non-uniform, anisotropic rods that may be naturally curved.

60. Stigter D: **Interactions of highly charged colloidal cylinders with applications to double-stranded DNA.** *Biopolymers* 1977, 16:1435–1448.

61. Brady GW, Sadowski M, Foos D, Benham CJ: **Environmental influences on DNA superhelicity. The effect of ionic strength on superhelix conformation in solution.** *J Mol Biol* 1987, 195:185–191.

62. Kraulis PJ: **MOLSCRIPT: a program to produce both detailed and schematic plots of protein structures.** *J Appl Crystallogr* 1991, 24:946–950.

T Schlick, New York University and The Howard Hughes Medical Institute, Department of Chemistry and The Courant Institute of Mathematical Sciences, 251 Mercer Street, New York, NY 10012-1185, USA. E-mail: schlick@nyu.edu